Force Computation for Dielectrics using Shape Calculus

P. Panchal and N. Ren and R. Hiptmair

Force Computation for Dielectrics using Shape Calculus

Piyush Panchal, Ning Ren, Ralf Hiptmair

May 20, 2022

Abstract

We are concerned with the numerical computation of electrostatic forces/torques in only piecewise homogeneous materials using the boundary element method (BEM). Conventional force formulas based on the Maxwell stress tensor yield functionals that fail to be continuous on natural trace spaces. Thus their use in conjunction with BEM incurs slow convergence and low accuracy. We employ the remedy discovered in [P. PANCHAL AND R. HIPTMAIR, *Electrostatic Force Computation with Boundary Element Methods*, The SMAI journal of computational mathematics, 8 (2022), pp. 49–74]: Motivated by the virtual work principle which is interpreted using techniques of shape calculus, and using the the adjoint method from shape optimization, we derive stable interface-based force functionals suitable for use with BEM. This is done in the framework of single-trace direct boundary integral equations for second-order transmission problems. Numerical tests confirm the fast asymptotic convergence and superior accuracy of the new formulas for the computation of total forces and torques.

1 Introduction

1.1 Topic and Goals

When a body composed of several homogeneous dielectrics is exposed to an electric field, it will experience forces, which are concentrated at the material interfaces. Since these forces induce mechanical stress, they represent important quantities of interest in the numerical simulation of electromagnetic phenomena.

The Maxwell stress tensor supplies the classical formulas for electromagnetic force densities [14, Sec. 6.9],[7, Sec. 8.2]. For piecewise homogeneous media these formulas can even be reduced to expressions entirely relying on restrictions of the fields to interfaces. However, these expressions are affected by intrinsic instability, because they fail to provide functionals that are continuous in energy trace spaces. As a consequence, when they are used with numerically computed approximations of the fields, they offer only low accuracy, in particular when the fields feature singularities. For volume-based discretization techniques like the finite element method (FEM) a simple remedy is to avoid using interfaced-based formulas and employ equivalent volume-based expressions instead. Those are perfectly stable and yield highly accurate forces, which even enjoy "superconvergence" when used with the FEM.

The use of volume-based force formulas is not an option when using the boundary element method (BEM) for the approximate computation of the electric field. Remember that that method is based on reformulations of the electrostatic transmission problem as integral equations posed in traces spaces on material interfaces. This means that the BEM directly approximates traces or jumps of fields on interfaces and dispenses with meshing the volume. Thus, using

stable volume-based force formulas is not feasible with reasonable effort. Can we avoid using the unstable interface-based force formulas in the context of BEM?

In this article we demonstrate that the answer is yes. By harnessing the virtual work principle we devise a stable way to compute forces directly from approximate solutions of boundary integral equations. It is stable in the sense that the resulting force functionals are continuous on energy-related trace spaces on interfaces. Thus, we can benefit from the extraordinary accuracy and fast convergence offered by continuous output functionals in conjunction with Galerkin discretization [17, Prop. 1.2]. The mathematical tools that paved the way for the new better force formulas are shape calculus, transformation techniques using suitable pullbacks of traces, and the adjoint method borrowed from constrained optimization.

1.2 Electrostatic Transmission Model Problem

To keep the presentation focused we confine ourselves to the following setting: We consider a parallel-plate capacitor where the gap between the plates is filled with two homogeneous, isotropic, and linear dielectric materials. The gap between the plates, containing both dielectrics, is denoted by the simply connected, open Lipschitz domain $\Omega \subset \mathbb{R}^d$, $d = 2, 3$. The dielectric materials are referred to by an index $i \in \{1, 2\}$ and the corresponding dielectric tensors are given as $\boldsymbol{\varepsilon}_i = \varepsilon_i \, \mathbf{I}_d$, where $\varepsilon_i \in \mathbb{R}^+$ is a constant and $\mathbf{I}_d$ is the $d \times d$ identity matrix. Dielectric 1 occupies the open, connected, Lipschitz domain $\Omega_1 \subset \Omega$ whereas dielectric 2 occupies the open, Lipschitz domain $\Omega_2 \subset \Omega$ such that $\overline{\Omega}_1 \cup \Omega_2 = \Omega$ and $\overline{\Omega}_1 \cap \overline{\Omega}_2 = \partial \Omega_1$. In other words, Dielectric 1 is embedded inside Dielectric 2 as shown in Figure 1. Under operation of the capacitor, there is an imposed potential difference between the plates, giving rise to an electric field in Ω which stores energy.

We use the notation $\Gamma_I := \partial \Omega_1$ for the interface between two dielectrics, $\Gamma_D \subset \partial \Omega$ for the edges of Dielectric 2 touching the capacitor plates where the external voltage is applied and $\Gamma_N := \partial \Omega \setminus \Gamma_D$ for the free boundary of capacitor, as shown in Figure 1. In the sequel we admit a more general Dirichlet boundary condition $\mathfrak{g} \in H^{\frac{1}{2}}(\Gamma_D)$. On the boundary Γ_N a zero Neumann boundary condition is a sensible choice to model the ideal case where the electric field lines stay inside the dielectric and there is no fringing around the edges [7, Section 4.4]. Also here we may impose a more general Neumann boundary condition through a function $\eta \in H^{-\frac{1}{2}}(\Gamma_N)$.

Writing $\boldsymbol{n}_2$ for the exterior unit normal vector field on $\partial \Omega_2$, the electrostatic scalar potential $u : \Omega \to \mathbb{R}$ can be obtained as the weak solution in $H^1(\Omega)^1$ of the linear elliptic mixed boundary value problem

$$\nabla \cdot (\boldsymbol{\varepsilon} \nabla u) = 0 \quad \text{in} \quad \Omega, \quad u = \mathfrak{g} \quad \text{on} \quad \Gamma_D, \quad \nabla u \cdot \boldsymbol{n}_2 = \eta \quad \text{on} \quad \Gamma_N, \tag{1}$$

where $\boldsymbol{\varepsilon}(\boldsymbol{x}) = \boldsymbol{\varepsilon}_i$, for $\boldsymbol{x} \in \Omega_i$, $i = 1, 2$. Due to the presence of two different media in our domain, the problem (1) can be reformulated as a transmission problem. Using the notation u_i for the potential solution inside Ω_i and $\boldsymbol{n}_1$ for the exterior unit normal field for $\partial \Omega_1$, we get two Laplace problems

$$\Delta u_1 = 0 \quad \text{in} \quad \Omega_1, \tag{2}$$

and

$$\Delta u_2 = 0 \quad \text{in} \quad \Omega_2, \quad u_2 = \mathfrak{g} \quad \text{on} \quad \Gamma_D, \quad \nabla u_2 \cdot \boldsymbol{n}_2 = \eta \quad \text{on} \quad \Gamma_N. \tag{3}$$

The potential solutions in the two domains are connected via two transmission conditions [18, Sec. 1.1] at the interface Γ_I which are given as

$$u_1|_{\Gamma_I} = u_2|_{\Gamma_I}, \quad \varepsilon_1 \, \nabla u_1 \cdot \boldsymbol{n}_1|_{\Gamma_I} = -\varepsilon_2 \, \nabla u_2 \cdot \boldsymbol{n}_2|_{\Gamma_I}. \tag{4}$$

---

[1]We adopt the convention of [18, Sec. 2.3 & Sec. 2.4] for function spaces and Sobolev spaces: $W^{k,p}(\Omega), H^1(\Omega), H^{\frac{1}{2}}(\Omega), L^2(\Omega), C^k(\Omega)$ etc., where Ω denotes a generic domain.
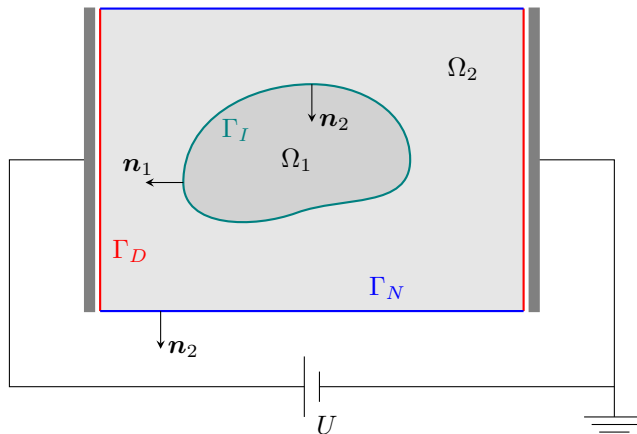
Figure 1: Geometric setting for model problem

1.3 Novelty and Outline

This article is intended as a supplement and extension for our foundational work [17], where the main ideas and arguments have been elaborated for the case of electromagnetic forces on perfectly conducting bodies, which gives rise to Dirichlet boundary value problems. The transmission problems treated in the present work involve both Dirichlet and Neumann traces and significantly more complex boundary integral equations comprising all four fundamental boundary integral operators (BIOs), not just the simple single-layer BIO faced in [17]. Thus, this work entails more careful considerations as regards suitable pullbacks and some technical innovations, in particular concerning the hyper-singular BIO.

In the next section we give details about the boundary-element discretization of the transmission problem (1). We rely on the so-called direct single-trace boundary integral formulation (STF) [3], which features both Neumann and Dirichlet traces of the potential u as unknowns. The BEM produces piecewise polynomial approximations of those two traces, which, in principle, can be plugged into the conventional interface-based force formula, see Section 2.3, with disappointing results, however, as we will demonstrate in Section 4.

Section 3 is the core of the paper. Along the lines of [17, Sects. 3 & 4] we derive the new stable interface-based force formula (27) from the boundary integral equations in variational form. We emphasize that this rather involved derivation is the main focus of the present article. For the sake of brevity we will not dwell long on the continuity properties of the obtained functionals, but merely sketch the arguments in Section 3.6. For a more profound exposition refer to [17, Sect. 4].

In the final Section 4 we put the new formulas to test in a number of numerical experiments in two dimensions. For smooth and non-smooth interfaces we study the discretization error for total forces and torques. Without exaggeration, for all test cases our new force formulas perform vastly better than the classical interface-based expressions. They provide superior accuracy and enhanced rates of convergence under mesh refinement, clearly on par with what we get from volume-based formulas in the FEM.

2 Boundary Element Method

Now we introduce the relevant boundary integral equations. Since we have two Laplace problems on domains Ω_1 and Ω_2, we review the fundamental boundary integral equations for the Laplace operator.

2.1 Boundary Integral Equations (BIEs)

For a bounded open Lipschitz domain $\Theta \subset \mathbb{R}^d$, a function $u \in H^1(\Theta)$ weakly satisfying the Laplace equation $\Delta u = 0$ in Θ also satisfies the following equations:

$$\begin{bmatrix} -\mathrm{V} & \frac{Id}{2} + \mathrm{K} \\ \frac{Id}{2} - \mathrm{K}' & -\mathrm{W} \end{bmatrix} \begin{bmatrix} \mathrm{T}_N\, u \\ \mathrm{T}_D\, u \end{bmatrix} = \begin{bmatrix} 0 \\ 0 \end{bmatrix}. \tag{5}$$

In the equations above $\mathrm{T}_N : H^1(\Theta) \to H^{-\frac{1}{2}}(\partial\Theta)$ is the interior Neumann Trace operator and $\mathrm{T}_D : H^1(\Theta) \to H^{\frac{1}{2}}(\partial\Theta)$ is the interior Dirichlet Trace operator defined for smooth functions as:

$$\mathrm{T}_N\, u(\boldsymbol{x}^*) := \lim_{\boldsymbol{x} \in \Theta \to \boldsymbol{x}^* \in \partial\Theta} \nabla u(\boldsymbol{x}) \cdot \boldsymbol{n}(\boldsymbol{x}^*), \quad \mathrm{T}_D\, u(\boldsymbol{x}^*) := \lim_{\boldsymbol{x} \in \Theta \to \boldsymbol{x}^* \in \partial\Theta} u(\boldsymbol{x}), \tag{6}$$

where $\boldsymbol{n}$ is the unit exterior normal vector field on $\partial\Theta$. The operators V, K, K' and W are the well known Single layer, Double layer, Adjoint double layer and Hypersingular boundary integral operators (BIOs) from BEM theory, for which we refer to the textbooks [20, Ch. 6] [18, Ch. 3] where definitions of the Sobolev spaces $H^1(\Theta), H^{-\frac{1}{2}}(\partial\Theta)$ and its dual $H^{\frac{1}{2}}(\partial\Theta)$ can also be found. These BIOs are bounded linear operators acting between the following spaces:

$$\mathrm{V} : H^{-\frac{1}{2}}(\partial\Theta) \to H^{\frac{1}{2}}(\partial\Theta), \qquad\qquad \mathrm{K} : H^{\frac{1}{2}}(\partial\Theta) \to H^{\frac{1}{2}}(\partial\Theta),$$
$$\mathrm{K}' : H^{-\frac{1}{2}}(\partial\Theta) \to H^{-\frac{1}{2}}(\partial\Theta), \qquad\qquad \mathrm{W} : H^{\frac{1}{2}}(\partial\Theta) \to H^{-\frac{1}{2}}(\partial\Theta).$$

2.2 Variational Boundary Integral Equations

We have two sets of boundary integral equations on two dielectric domains Ω_i, $i = 1, 2$. Combining them with the transmission conditions, we obtain well posed boundary integral equations (BIEs). The two sets of BIEs can be compactly written as

$$\begin{bmatrix} -\mathrm{V}_i & \frac{Id}{2} + \mathrm{K}_i \\ \frac{Id}{2} - \mathrm{K}_i' & -\mathrm{W}_i \end{bmatrix} \begin{bmatrix} \mathrm{T}_N^i\, u_i \\ \mathrm{T}_D^i\, u_i \end{bmatrix} = \begin{bmatrix} 0 \\ 0 \end{bmatrix}, \tag{7}$$

where the subscript i in the BIOs denote that they are defined on the boundary $\partial\Omega_i$ and the corresponding trace operators are denoted by the superscript i, defined by replacing $\Theta \to \Omega_i$ and $\partial\Theta \to \partial\Omega_i$ in (6).

To obtain a variational formulation, we first rely on the offset function technique used for mixed boundary value problem [20, Ch. 7][18, Ch. 4]. Let $\mathfrak{g}' \in H^{\frac{1}{2}}(\partial\Omega)$ and $\eta' \in H^{-\frac{1}{2}}(\partial\Omega)$ be suitable extensions of the given boundary traces $\mathfrak{g}$ and η respectively such that $\mathfrak{g}'|_{\Gamma_D} = \mathfrak{g}$ and $\eta'|_{\Gamma_N} = \eta$. Using these extensions, we can write the traces[2] on $\partial\Omega$ as:

$$\begin{aligned} \mathrm{T}_D^2\, u_2\big|_{\partial\Omega} &:= \mathfrak{g}' + \mathfrak{u}, \quad \mathfrak{u} \in \tilde{H}^{\frac{1}{2}}(\Gamma_N) := \{ \mathfrak{v} \in H^{\frac{1}{2}}(\partial\Omega) : \mathrm{supp}(\mathfrak{v}) \subset \Gamma_N \}, \\ \mathrm{T}_N^2\, u_2\big|_{\partial\Omega} &:= \eta' + \psi, \quad \psi \in \tilde{H}^{-\frac{1}{2}}(\Gamma_D) := \{ \phi \in H^{-\frac{1}{2}}(\partial\Omega) : \mathrm{supp}(\mathfrak{v}) \subset \Gamma_D \}. \end{aligned} \tag{8}$$

---

[2]For functions in $H^{\frac{1}{2}}$ we use Roman letters and for those in $H^{-\frac{1}{2}}$ we use Greek letters

Traces on Γ_I are denoted as $\mathfrak{u}_I := \mathrm{T}_D^2 \, u_2 \big|_{\Gamma_I}$ and $\psi_I := \mathrm{T}_N^2 \, u_2 \big|_{\Gamma_I}$, where $\mathfrak{u}_I \in H^{\frac{1}{2}}(\Gamma_I)$ and $\psi_I \in H^{-\frac{1}{2}}(\Gamma_I)$. The task of solving the transmission problem (3) then becomes finding the unknown traces $\mathfrak{u} \in \tilde{H}^{\frac{1}{2}}(\Gamma_N)$, $\psi \in \tilde{H}^{-\frac{1}{2}}(\Gamma_D)$, $\mathfrak{u}_I \in H^{\frac{1}{2}}(\Gamma_I)$ and $\psi_I \in H^{-\frac{1}{2}}(\Gamma_I)$. More information on the "tilde spaces" can be found in literature [18, Sec. 2.4.2],[20, Sec. 2.5].

To get the variational equations we rely on the duality of the Sobolev spaces $H^{-\frac{1}{2}}$ and $H^{\frac{1}{2}}$. Multiplying the first equation in (7) for Ω_2 with some $\phi \in H^{-\frac{1}{2}}(\partial\Omega_2)$ and integrating, we get

$$\mathrm{a}_{\mathrm{V}_2}(\mathrm{T}_N^2 \, u_2, \phi) = \frac{1}{2} \left\langle \mathrm{T}_D^2 \, u_2, \phi \right\rangle_{L^2(\partial\Omega_2)} + \mathrm{a}_{\mathrm{K}_2}(\mathrm{T}_D^2 \, u_2, \phi) \quad \forall \phi \in H^{-\frac{1}{2}}(\partial\Omega_2), \tag{9}$$

where $\langle \cdot, \cdot \rangle_{L^2(\partial\Omega_2)}$ is the L^2 duality pairing and the bilinear forms are defined as:

$$\mathrm{a}_{\mathrm{V}_i} : \begin{cases} H^{-\frac{1}{2}}(\partial\Omega_i) \times H^{-\frac{1}{2}}(\partial\Omega_i) \to \mathbb{R} \\ \mathrm{a}_{\mathrm{V}_i}(\psi, \phi) := \left\langle \mathrm{V}_i \, \psi, \phi \right\rangle_{L^2(\partial\Omega_i)} = \displaystyle\int\limits_{\partial\Omega_i} \int\limits_{\partial\Omega_i} \mathrm{G}^\Delta(\boldsymbol{x}, \boldsymbol{y}) \, \psi(\boldsymbol{y}) \, \phi(\boldsymbol{x}) \, d\mathrm{S}(\boldsymbol{y}) d\mathrm{S}(\boldsymbol{x}), \end{cases}$$

$$\mathrm{a}_{\mathrm{K}_i} : \begin{cases} H^{\frac{1}{2}}(\partial\Omega_i) \times H^{-\frac{1}{2}}(\partial\Omega_i) \to \mathbb{R} \\ \mathrm{a}_{\mathrm{K}_i}(g, \phi) := \left\langle \mathrm{K}_i \, g, \phi \right\rangle_{L^2(\partial\Omega_i)} = \displaystyle\int\limits_{\partial\Omega_i} \int\limits_{\partial\Omega_i} \nabla_y \mathrm{G}^\Delta(\boldsymbol{x}, \boldsymbol{y}) \cdot \boldsymbol{n}_i(\boldsymbol{y}) \, g(\boldsymbol{y}) \, \phi(\boldsymbol{x}) d\mathrm{S}(\boldsymbol{y}) d\mathrm{S}(\boldsymbol{x}), \end{cases}$$

$i \in \{1, 2\}$, where $\mathrm{G}^\Delta(\boldsymbol{x}, \boldsymbol{y}) : \{(\boldsymbol{x}, \boldsymbol{y}) \in \mathbb{R}^d \times \mathbb{R}^d : \boldsymbol{x} \neq \boldsymbol{y}\} \to \mathbb{R}$ is the fundamental solution for the Laplace operator

$$\mathrm{G}^\Delta(\boldsymbol{x}, \boldsymbol{y}) := -\frac{1}{2\pi} \log(\|\boldsymbol{x} - \boldsymbol{y}\|) \quad \text{for } d = 2, \quad \mathrm{G}^\Delta(\boldsymbol{x}, \boldsymbol{y}) := \frac{1}{4\pi \, \|\boldsymbol{x} - \boldsymbol{y}\|} \quad \text{for } d = 3.$$

Let the chosen test function ϕ in (9) be such that $\phi|_{\Gamma_I} \equiv 0$, and $\phi|_{\partial\Omega} = \tilde{\phi} \in \tilde{H}^{-\frac{1}{2}}(\Gamma_D)$. The integrals over $\partial\Omega_2$ can be decomposed into integrals over the disjoint boundaries Γ_I and $\partial\Omega$ and we get

$$\int\limits_{\partial\Omega} \int\limits_{\Gamma_I} \mathrm{G}^\Delta(\boldsymbol{x}, \boldsymbol{y}) \, \psi_I(\boldsymbol{y}) \, \tilde{\phi}(\boldsymbol{x}) \, d\mathrm{S}(\boldsymbol{y}) d\mathrm{S}(\boldsymbol{x}) + \int\limits_{\partial\Omega} \int\limits_{\partial\Omega} \mathrm{G}^\Delta(\boldsymbol{x}, \boldsymbol{y}) \, (\eta'(\boldsymbol{y}) + \psi(\boldsymbol{y})) \, \tilde{\phi}(\boldsymbol{x}) \, d\mathrm{S}(\boldsymbol{y}) d\mathrm{S}(\boldsymbol{x})$$

$$= \frac{1}{2} \int\limits_{\partial\Omega} \mathfrak{g}'(\boldsymbol{x}) \, \tilde{\phi}(\boldsymbol{x}) \, d\mathrm{S}(\boldsymbol{x}) + \int\limits_{\partial\Omega} \int\limits_{\Gamma_I} \nabla_y \mathrm{G}^\Delta(\boldsymbol{x}, \boldsymbol{y}) \cdot \boldsymbol{n}_2(\boldsymbol{y}) \, \mathfrak{u}_I(\boldsymbol{y}) \, \tilde{\phi}(\boldsymbol{x}) \, d\mathrm{S}(\boldsymbol{y}) d\mathrm{S}(\boldsymbol{x})$$

$$+ \int\limits_{\partial\Omega} \int\limits_{\partial\Omega} \nabla_y \mathrm{G}^\Delta(\boldsymbol{x}, \boldsymbol{y}) \cdot \boldsymbol{n}_2(\boldsymbol{y}) \, (\mathfrak{u}(\boldsymbol{y}) + \mathfrak{g}'(\boldsymbol{y})) \, \tilde{\phi}(\boldsymbol{x}) \, d\mathrm{S}(\boldsymbol{y}) d\mathrm{S}(\boldsymbol{x}). \quad \forall \tilde{\phi} \in \tilde{H}^{-\frac{1}{2}}(\Gamma_D) \tag{10}$$

By introducing abbreviations for the double integrals that we encounter, the variational equations

can be written in a compact way

$$
a_V^{\bullet,\blacktriangle} : \begin{cases} H^{-\frac{1}{2}}(\Gamma_\bullet) \times H^{-\frac{1}{2}}(\Gamma_\blacktriangle) \to \mathbb{R} \\ \qquad\qquad (\psi,\phi) \mapsto \int\limits_{\Gamma_\blacktriangle} \int\limits_{\Gamma_\bullet} G^\Delta(\boldsymbol{x},\boldsymbol{y})\,\psi(\boldsymbol{y})\,\phi(\boldsymbol{x})\,dS(\boldsymbol{y})dS(\boldsymbol{x}). \end{cases}
$$

$$
l^\bullet : \begin{cases} H^{\frac{1}{2}}(\Gamma_\bullet) \times H^{-\frac{1}{2}}(\Gamma_\bullet) \to \mathbb{R} \\ \qquad\qquad (g,\phi) \mapsto \int\limits_{\Gamma_\bullet} g(\boldsymbol{x})\,\phi(\boldsymbol{x})\,dS(\boldsymbol{x}) \end{cases}
$$

$$
a_K^{\bullet,\blacktriangle} : \begin{cases} H^{\frac{1}{2}}(\Gamma_\bullet) \times H^{\frac{1}{2}}(\Gamma_\blacktriangle) \to \mathbb{R} \\ \qquad\qquad (g,\phi) \mapsto \int\limits_{\Gamma_\blacktriangle} \int\limits_{\Gamma_\bullet} \nabla_y G^\Delta(\boldsymbol{x},\boldsymbol{y}) \cdot \boldsymbol{n}_2(\boldsymbol{y})\,g(\boldsymbol{y})\,\phi(\boldsymbol{x})\,dS(\boldsymbol{y})dS(\boldsymbol{x}) \end{cases}
$$

$$
a_W^{\bullet,\blacktriangle} : \begin{cases} H^{\frac{1}{2}}(\Gamma_\bullet) \times H^{\frac{1}{2}}(\Gamma_\blacktriangle) \to \mathbb{R} \\ \qquad\qquad (g,v) \mapsto \int\limits_{\Gamma_\blacktriangle} \int\limits_{\Gamma_\bullet} G^\Delta(\boldsymbol{x},\boldsymbol{y})\,\dfrac{d}{dt}g(\boldsymbol{y})\,\dfrac{d}{dt}v(\boldsymbol{x})\,dS(\boldsymbol{y})dS(\boldsymbol{x}) \qquad\qquad\text{(2D)} \\ \qquad\qquad (g,v) \mapsto \int\limits_{\Gamma_\blacktriangle} \int\limits_{\Gamma_\bullet} G^\Delta(\boldsymbol{x},\boldsymbol{y})\,\mathbf{curl}_\Gamma\,g(\boldsymbol{y}) \cdot \mathbf{curl}_\Gamma\,v(\boldsymbol{x})\,dS(\boldsymbol{y})dS(\boldsymbol{x}) \qquad\text{(3D)}. \end{cases}
$$

where $\bullet, \blacktriangle \in \{I, G\}$, $\Gamma_G := \partial\Omega$ and $\mathbf{curl}_\Gamma\,u(\boldsymbol{x}) := \mathbf{grad}_\Gamma\,u(\boldsymbol{x}) \times \boldsymbol{n}_2(\boldsymbol{x})$, where $\mathbf{grad}_\Gamma$ is the surface gradient operator. This notation allows us to rewrite (10) as

$$
a_V^{I,G}(\psi_I,\tilde{\phi}) + a_V^{G,G}(\psi,\tilde{\phi}) - a_K^{I,G}(u_I,\tilde{\phi}) - a_K^{G,G}(\mathfrak{u},\tilde{\phi})
$$
$$
= \frac{1}{2}l^G(\mathfrak{g}',\tilde{\phi}) - a_V^{G,G}(\eta',\tilde{\phi}) + a_K^{G,G}(\mathfrak{g}',\tilde{\phi}) \quad \forall\tilde{\phi} \in \tilde{H}^{-\frac{1}{2}}(\Gamma_D).
$$

Similarly testing the second equation in (7) for Ω_2 with a function $\mathfrak{v} \in H^{\frac{1}{2}}(\partial\Omega_2)$ with $\mathfrak{v}|_{\partial\Omega} = \tilde{\mathfrak{v}} \in \tilde{H}^{\frac{1}{2}}(\Gamma_N)$ and $\mathfrak{v}|_{\Gamma_I} \equiv 0$ we get the variational equation

$$
a_W^{I,G}(\mathfrak{u}_I,\tilde{\mathfrak{v}}) + a_W^{G,G}(\mathfrak{u},\tilde{\mathfrak{v}}) + a_K^{G,G}(\tilde{\mathfrak{v}},\psi) + a_K^{G,I}(\tilde{\mathfrak{v}},\psi_I)
$$
$$
= \frac{1}{2}l^G(\tilde{\mathfrak{v}},\eta') - a_W^{G,G}(\mathfrak{g}',\tilde{\mathfrak{v}}) - a_K^{G,G}(\tilde{\mathfrak{v}},\eta') \quad \forall\tilde{v} \in \tilde{H}^{\frac{1}{2}}(\Gamma_N).
$$

Note that we write the bilinear form corresponding to K' in terms of $a_K^{\bullet,\blacktriangle}$ as K' is the adjoint of the BIO K. Next we obtain equations for Γ_I. We test the first equation in (7) for Ω_1 with $\phi_I \in H^{-\frac{1}{2}}(\Gamma_I)$:

$$
a_{V_1}(T_N^1\,u_1, \phi_I) = \frac{1}{2}\left\langle T_D^1\,u_1, \phi_I \right\rangle_{L^2(\Gamma_I)} + a_{K_1}(T_D^1\,u_1, \phi_I) \quad \forall\phi_I \in H^{-\frac{1}{2}}(\Gamma_I). \tag{11}
$$

From the transmission conditions (4) we know that $\varepsilon_1\,T_N^1\,u_1 + \varepsilon_2\,T_N^2\,u_2 = 0$ on Γ_I, which gives $T_N^1\,u_1 = -\frac{\varepsilon_2}{\varepsilon_1}\psi_I$, and that $T_D^1\,u_1 = \mathfrak{u}_I$. Using these relations we get

$$
-\frac{\varepsilon_2}{\varepsilon_1} \int\limits_{\Gamma_I} \int\limits_{\Gamma_I} G^\Delta(\boldsymbol{x},\boldsymbol{y})\,\psi_I(\boldsymbol{y})\,\phi_I(\boldsymbol{x})\,dS(\boldsymbol{y})dS(\boldsymbol{x}) = \frac{1}{2} \int\limits_{\Gamma_I} \mathfrak{u}_I(\boldsymbol{x})\,\phi_I(\boldsymbol{x})\,dS(\boldsymbol{x})
$$
$$
+ \int\limits_{\Gamma_I} \int\limits_{\Gamma_I} \nabla G^\Delta(\boldsymbol{x},\boldsymbol{y}) \cdot \boldsymbol{n}_1(\boldsymbol{y})\,\mathfrak{u}_I(\boldsymbol{y})\,\phi_I(\boldsymbol{x})\,dS(\boldsymbol{y})dS(\boldsymbol{x}) \quad \forall\phi_I \in H^{-\frac{1}{2}}(\Gamma_I). \tag{12}
$$

6

These equations on Γ_I are not very useful by themselves, as we do not know any traces on Γ_I. We combine these equations with corresponding equations for Ω_2. For the first one we test the first equation (7) for Ω_2 with a function $\phi \in H^{-\frac{1}{2}}(\partial\Omega_2)$ such that $\phi|_{\partial\Omega} \equiv 0$ and $\phi|_{\Gamma_I} = \phi_I \in H^{-\frac{1}{2}}(\Gamma_I)$. Then combining it with (12) we get

$$a_V^{G,I}(\psi,\phi_I) + (1 + \frac{\varepsilon_2}{\varepsilon_1})a_V^{I,I}(\psi_I,\phi_I) - a_K^{G,I}(\mathfrak{u},\phi_I) - 2a_K^{I,I}(\mathfrak{u}_I,\phi_I) =$$
$$-a_V^{G,I}(\eta',\phi_I) + a_K^{G,I}(\mathfrak{g}',\phi_I) \quad \forall \phi_I \in H^{-\frac{1}{2}}(\Gamma_I).$$

We use a similar procedure to obtain the second equation

$$a_W^{G,I}(\mathfrak{u},\mathfrak{v}_I) + (1 + \frac{\varepsilon_1}{\varepsilon_2})a_W^{I,I}(\mathfrak{u}_I,\mathfrak{v}_I) + a_K^{I,G}(\mathfrak{v}_I,\psi) + 2a_K^{I,I}(\mathfrak{v}_I,\psi_I) =$$
$$-a_W^{G,I}(\mathfrak{g}',\mathfrak{v}_I) - a_K^{I,G}(\mathfrak{v}_I,\eta') \quad \forall \mathfrak{v}_I \in H^{\frac{1}{2}}(\Gamma_I).$$

In the combined system of equations we seek $\mathfrak{u} \in \tilde{H}^{\frac{1}{2}}(\Gamma_N)$, $\psi \in \tilde{H}^{-\frac{1}{2}}(\Gamma_D)$, $\mathfrak{u}_I \in H^{\frac{1}{2}}(\Gamma_I)$ and $\psi_I \in H^{-\frac{1}{2}}(\Gamma_I)$ such that

$$a_W^{G,I}(\mathfrak{u},\mathfrak{v}_I) + (1 + \frac{\varepsilon_1}{\varepsilon_2})a_W^{I,I}(\mathfrak{u}_I,\mathfrak{v}_I) + a_K^{I,G}(\mathfrak{v}_I,\psi) + 2a_K^{I,I}(\mathfrak{v}_I,\psi_I)$$
$$= -a_W^{G,I}(\mathfrak{g}',\mathfrak{v}_I) - a_K^{I,G}(\mathfrak{v}_I,\eta') \qquad \forall \mathfrak{v}_I \in H^{\frac{1}{2}}(\Gamma_I),$$
$$a_V^{G,I}(\psi,\phi_I) + (1 + \frac{\varepsilon_2}{\varepsilon_1})a_V^{I,I}(\psi_I,\phi_I) - a_K^{G,I}(\mathfrak{u},\phi_I) - 2a_K^{I,I}(\mathfrak{u}_I,\phi_I)$$
$$= -a_V^{G,I}(\eta',\phi_I) + a_K^{G,I}(\mathfrak{g}',\phi_I) \qquad \forall \phi_I \in H^{-\frac{1}{2}}(\Gamma_I),$$
$$a_V^{I,G}(\psi_I,\tilde{\phi}) + a_V^{G,G}(\psi,\tilde{\phi}) - a_K^{I,G}(u_I,\tilde{\phi}) - a_K^{G,G}(\mathfrak{u},\tilde{\phi})$$
$$= \frac{1}{2}l^G(\mathfrak{g}',\tilde{\phi}) - a_V^{G,G}(\eta',\tilde{\phi}) + a_K^{G,G}(\mathfrak{g}',\tilde{\phi}) \quad \forall \tilde{\phi} \in \tilde{H}^{-\frac{1}{2}}(\Gamma_D),$$
$$a_W^{I,G}(\mathfrak{u}_I,\tilde{\mathfrak{v}}) + a_W^{G,G}(\mathfrak{u},\tilde{\mathfrak{v}}) + a_K^{G,G}(\tilde{\mathfrak{v}},\psi) + a_K^{G,I}(\tilde{\mathfrak{v}},\psi_I)$$
$$= \frac{1}{2}l^G(\tilde{\mathfrak{v}},\eta') - a_W^{G,G}(\mathfrak{g}',\tilde{\mathfrak{v}}) - a_K^{G,G}(\tilde{\mathfrak{v}},\eta') \quad \forall \tilde{v} \in \tilde{H}^{\frac{1}{2}}(\Gamma_N).$$

(13)

Remark 1. From our knowledge of the mapping properties of the layer potentials and boundary integral operators [18, Sec. 3.1.2] we know that all the bilinear forms on the LHS of (13) are bounded. Combining all the bilinear forms on the LHS and setting $(\tilde{\mathfrak{v}}, \tilde{\phi}, \mathfrak{v}_I, \phi_I) = (\mathfrak{u}, \psi, \mathfrak{u}_I, \psi_I)$ we get the ellipticity estimate

$$(1 + \frac{\varepsilon_1}{\varepsilon_2})a_W^{I,I}(\mathfrak{u}_I,\mathfrak{u}_I) + (1 + \frac{\varepsilon_2}{\varepsilon_1})a_V^{I,I}(\psi_I,\psi_I) + a_V^{G,G}(\psi,\psi) + a_W^{G,G}(\mathfrak{u},\mathfrak{u}) + 2a_V^{I,G}(\psi_I,\psi) + 2a_W^{I,G}(\mathfrak{u}_I,\mathfrak{u})$$
$$\geq a_V^{I,I}(\psi_I,\psi_I) + a_V^{G,G}(\psi,\psi) + 2a_V^{I,G}(\psi_I,\psi) + a_W^{G,G}(\mathfrak{u},\mathfrak{u}) + 2a_W^{I,G}(\mathfrak{u}_I,\mathfrak{u}) + a_W^{I,I}(\mathfrak{u}_I,\mathfrak{u}_I)$$
$$= a_{V_2}(\psi',\psi') + a_{W_2}(\mathfrak{u}',\mathfrak{u}')$$
$$\geq c \left(\|\psi\|^2_{\tilde{H}^{-\frac{1}{2}}(\Gamma_D)} + \|\psi_I\|^2_{H^{-\frac{1}{2}}(\Gamma_I)} + \|\mathfrak{u}_I\|^2_{H^{\frac{1}{2}}(\Gamma_I)} + \|\mathfrak{u}\|^2_{\tilde{H}^{\frac{1}{2}}(\Gamma_N)} \right),$$

where $\psi' \in H^{-\frac{1}{2}}(\partial\Omega_2) : \psi'|_{\Gamma_I} = \psi_I, \psi'|_{\partial\Omega} = \psi$ and $\mathfrak{u}' \in H^{\frac{1}{2}}(\partial\Omega_2) : \mathfrak{u}'|_{\Gamma_I} = \mathfrak{u}_I, \mathfrak{u}'|_{\partial\Omega} = \mathfrak{u}$. For ellipticity results on the bilinear forms a_V and a_W we refer to [18, Sec. 3.5.2]. The existence of a unique solution for (13) is then guaranteed by the Lax-Milgram lemma [18, Lem. 2.1.51].

7

2.3 Boundary-Element Galerkin Discretization

We start with mesh partitions $\mathcal{M}_h$ and $\mathcal{N}_h$ of the boundaries $\partial\Omega$ and Γ_I respectively, whose cells consist of either curved segments $d = 2$ or curved triangular panels $d = 3$. We perform a Galerkin discretization of (13) employing the lowest order boundary element spaces $S_0^{-1}(\mathcal{M}_h)$ and $S_0^{-1}(\mathcal{N}_h)$ to approximate $H^{-\frac{1}{2}}(\partial\Omega)$ and $H^{-\frac{1}{2}}(\Gamma_I)$ respectively, and $S_1^0(\mathcal{M}_h)$ and $S_1^0(\mathcal{N}_h)$ to approximate $H^{\frac{1}{2}}(\partial\Omega)$ and $H^{\frac{1}{2}}(\Gamma_I)$ respectively. For notations and details about the construction of the spaces S_q^{-1} and S_q^0 we refer to [20, Ch. 10] or [18, Ch. 4]. The choice of basis functions and the computation of the Galerkin matrices is presented in [18, Ch. 5].

2.4 Using Interface-Based Force Formulas with BEM

Classical methods for computing electrostatic forces rely on the Maxwell stress tensor[3][7, Section 8.2, Eq. 8.17]. For a linear, homogeneous, and isotropic dielectric medium with permittivity ε and a static electric field, the Maxwell stress tensor is defined as

$$\mathbf{T}(u)(\boldsymbol{x}) := \varepsilon \left(\nabla u(\boldsymbol{x}) \nabla u(\boldsymbol{x})^\top - \frac{1}{2} \|\nabla u(\boldsymbol{x})\|^2 \mathbf{I}_d \right), \quad \boldsymbol{x} \in \Omega, \tag{14}$$

where $u(\boldsymbol{x})$ is the electrostatic potential inside Ω. At a material interface Γ, the Maxwell stress tensor is generally discontinuous and the surface force density $\mathbf{f}^\Gamma$ is defined as $[\mathbf{T}(u)]\boldsymbol{n}_1$ [11] where $[\mathbf{T}(u)]$ is the jump of the Maxwell stress tensor across the interface Γ_I, defined as outside minus inside and $\boldsymbol{n}_1$ is the exterior unit normal vector field on Γ. For Dielectric 1 in our model problem, there are no residual charges inside the body Ω_1, hence it experiences only surface forces. The net force $\mathbf{F}$ on Γ_I can be obtained by integrating the surface force density

$$\mathbf{F} := \int_{\Gamma_I} \mathbf{f}^\Gamma(\boldsymbol{x}) \, \mathrm{d}S(\boldsymbol{x}) = \int_{\Gamma_I} \left(\mathbf{T}(u_2)(\boldsymbol{x}) - \mathbf{T}(u_1)(\boldsymbol{x}) \right) \boldsymbol{n}_1(\boldsymbol{x}) \, \mathrm{d}S(\boldsymbol{x}). \tag{15}$$

Note that the above expression for net force is an interface-based expression as it only involves integration on the boundary Γ_I.

The computed Galerkin solutions $\mathfrak{u}_I^h, \psi_I^h, \mathfrak{u}^h$ and ψ^h can be plugged into the interface-based formula (15) to get an approximation of the net force. To use the computed traces directly, we use a simplified version of the boundary formula for $d = 2$, which can be obtained by using the transmission conditions:

$$\mathbf{F} = \frac{\varepsilon_1 - \varepsilon_2}{2} \int_{\Gamma_I} \left(\left(\frac{d\mathfrak{u}_I}{dt}(\boldsymbol{x}) \right)^2 + \frac{\varepsilon_2}{\varepsilon_1} \psi_I^2(\boldsymbol{x}) \right) \boldsymbol{n}_1(\boldsymbol{x}) \, \mathrm{d}S(\boldsymbol{x}), \tag{16}$$

where $\frac{d\mathfrak{u}_I}{dt}$ represents the arclength derivative of $\mathfrak{u}_I$. The approximate force $\mathbf{F}_{BEM}^h$ is then given as

$$\mathbf{F}_{BEM}^h = \frac{\varepsilon_1 - \varepsilon_2}{2} \int_{\Gamma_I} \left(\left(\frac{d\mathfrak{u}_I^h}{dt}(\boldsymbol{x}) \right)^2 + \frac{\varepsilon_2}{\varepsilon_1} (\psi_I^h(\boldsymbol{x}))^2 \right) \boldsymbol{n}_1(\boldsymbol{x}) \, \mathrm{d}S(\boldsymbol{x}) \tag{17}$$

Note that the expression is not well defined on $H^{\frac{1}{2}}(\Gamma_I) \times H^{-\frac{1}{2}}(\Gamma_I)$, which reflects its inherent instability pointed out in the Introduction.

---

[3]$\mathbf{I}_d$ stands for the $d \times d$ identity matrix, $\|.\|$ denotes the Euclidean norm

3 Forces via Shape Differentiation

3.1 Virtual Work Principle

The Virtual Work Principle [11, 4, 2, 12, 1] tells us that the force can be recovered via the shape derivative of the total energy. We will first introduce tools from Shape Calculus to give a precise meaning to differentiating with respect to a shape and then apply them to our electrostatic setting introduced in Section 1.2.

We start with a nonempty subset $D \subset \mathbb{R}^d$ which will be the hold-all domain. We denote by $P(D)$ the set of all subsets of D. Let $\mathcal{A} \subset P(D)$ be a family of admissible domains. A shape functional is then a map $J : \mathcal{A} \to \mathbb{R}$, $\Omega \in \mathcal{A} \mapsto J(\Omega)$. To differentiate the shape functional $J(\Omega)$ with respect to Ω, we use the perturbation method from literature [19, Sect. 2.8]. Starting from a perturbation field $\boldsymbol{\nu} \in C_0^\infty(D; \mathbb{R}^d)$, compactly supported in the hold-all domain D we define the perturbation map

$$\mathrm{T}_{\boldsymbol{\nu}}^s : D \to \mathbb{R}^d, \quad \mathrm{T}_{\boldsymbol{\nu}}^s(\boldsymbol{x}) := \boldsymbol{x} + s\,\boldsymbol{\nu}(\boldsymbol{x}), \quad s \in \mathbb{R}. \tag{18}$$

The implicit function theorem ensures that there is a $\delta = \delta(\boldsymbol{\nu})$ such that $\mathrm{T}_{\boldsymbol{\nu}}^s$ is a C^∞ diffeomorphism, if $|s| < \delta(\boldsymbol{\nu})$. The shape derivative is defined as the limit

$$\frac{dJ}{d\Omega}(\Theta; \boldsymbol{\nu}) := \lim_{s \to 0} \frac{J(\mathrm{T}_{\boldsymbol{\nu}}^s(\Theta)) - J(\Theta)}{s},$$

if it exists. It is called the shape (Gateaux) derivative of J at $\Theta \in \mathcal{A}$ in the direction $\boldsymbol{\nu}$. If, in addition, $\boldsymbol{\nu} \to \frac{dJ}{d\Omega}(\Theta; \boldsymbol{\nu}) \in \mathbb{R}$ is a distribution on the space of test velocity fields $C_0^\infty(D; \mathbb{R}^d)$, a 1-current as called by de Rham [5, Ch. 3, § 8] then $\Omega \mapsto J(\Omega)$ is called shape-differentiable at Θ and that distribution is the shape derivative.

Remark 2. The Hadamard structure theorem [6, Ch. 9, Thm 3.6] states that for domains Θ with C^∞ boundary, the shape derivative $\boldsymbol{\nu} \mapsto \frac{dJ}{d\Omega}(\Theta; \boldsymbol{\nu})$ admits a representative f in the space of distributions on $C^\infty(\partial\Theta)$

$$\frac{dJ}{d\Omega}(\Theta; \boldsymbol{\nu}) = \langle f, \boldsymbol{\nu} \cdot \boldsymbol{n}|_{\partial\Theta} \rangle, \quad \boldsymbol{\nu} \in C_0^\infty(D; \mathbb{R}^d).$$

The distribution can be regarded as representing a normal surface force density.

3.2 BIEs on Perturbed Interface

The perturbation map (18) gives a set of admissible domains $\mathcal{A}_{\boldsymbol{\nu}}$, which is constructed using perturbations of a reference domain $\Omega_0 \subset D$, that is $\mathcal{A}_{\boldsymbol{\nu}} := \{\Omega_s := \mathrm{T}_{\boldsymbol{\nu}}^s(\Omega_0), s \in (-\delta(\boldsymbol{\nu}), \delta(\boldsymbol{\nu}))\}$. In spirit of the Virtual Work Principle, we consider our electrostatic setting from Section 1.2 on this set of admissible domains. Note that the chosen velocity field $\boldsymbol{\nu}$ is compactly supported on the hold-all domain D and not the capacitor boundary $\partial\Omega_0$. For computing forces on the interface Γ_I^0 we need $\boldsymbol{\nu}$ it to be compactly supported on Ω_0 but we admit a more general perturbation field at this point and will only make the simplification later on.

For the "s" configuration, all the boundaries and interfaces relevant to the weak BIE formulation in Section 2 are defined using the perturbation map, the dielectric constant $\varepsilon_s(\boldsymbol{x}) := \varepsilon_i$ for $\boldsymbol{x} \in \Omega_i^s$, and the boundary conditions are denoted by $\mathfrak{g}_s' \in H^{\frac{1}{2}}(\partial\Omega_s)$ and $\eta_s' \in H^{-\frac{1}{2}}(\partial\Omega_s)$. We define the total energy functional $\mathcal{J}(s)$ as the sum of battery's energy $\mathcal{J}_B(s)$ and the electric field

energy $\mathcal{J}_F(s)$, where $\mathcal{J}, \mathcal{J}_B, \mathcal{J}_F : (-\delta(\boldsymbol{\nu}), \delta(\boldsymbol{\nu})) \to \mathbb{R}$ and the field energy functional is defined as

$$
\begin{aligned}
\mathcal{J}_F(s) &:= \frac{1}{2} \int\limits_{\Omega_s} \varepsilon_s(\boldsymbol{x}) \nabla u_s(\boldsymbol{x}) \cdot \nabla u_s(\boldsymbol{x}) \, d\mathrm{S}(\boldsymbol{x}) \\
&= \frac{\varepsilon_1}{2} \int\limits_{\Omega_1^s} ||\nabla u_1^s(\boldsymbol{x})||^2 \, d\mathrm{S}(\boldsymbol{x}) + \frac{\varepsilon_2}{2} \int\limits_{\Omega_2^s} ||\nabla u_2^s(\boldsymbol{x})||^2 \, d\mathrm{S}(\boldsymbol{x}) \\
&= \frac{\varepsilon_2}{2} \int\limits_{\partial\Omega_s} (\mathfrak{u}_s(\boldsymbol{x}) + \mathfrak{g}_s'(\boldsymbol{x})) \, (\eta_s'(\boldsymbol{x}) + \psi_s(\boldsymbol{x})) \, d\mathrm{S}(\boldsymbol{x}) =: J(s; \mathfrak{u}_s, \psi_s),
\end{aligned}
\tag{19}
$$

where the functions with "s" sub/super-scripts are the solutions in the "s" configuration.

Remark 3. The shape derivative of battery's energy $\frac{d\mathcal{J}_B}{ds}(0) = -2\frac{d\mathcal{J}_F}{ds}(0)$ since it is given as $U\frac{dQ}{ds}(0)$, where $Q(s)$ is the net charge on the outer boundary $\partial\Omega_s$ and U is the constant voltage drop [17, Rem. 3.1]. Hence we only need to examine the shape derivative of the field energy which gives the negative force field.

Since the perturbation map is a C^∞ diffeomorphism for small enough s, the domains in $\mathcal{A}_{\boldsymbol{\nu}}$ will possess connected, Lipschitz boundaries. We use the same formulation from (13) and replace Ω by Ω_s. To account for this additional s dependence that now shows up through Ω_s, we augment our notation for (bi)linear forms:

$$
\mathrm{a}_{\mathrm{V}}^{\bullet, \blacktriangle}(s) : \begin{cases} H^{-\frac{1}{2}}(\mathrm{T}_{\boldsymbol{\nu}}^s(\Gamma_\bullet^0)) \times H^{-\frac{1}{2}}(\mathrm{T}_{\boldsymbol{\nu}}^s(\Gamma_\blacktriangle^0)) \to \mathbb{R} \\ \mathrm{a}_{\mathrm{V}}^{\bullet, \blacktriangle}(s; \psi, \phi) := \displaystyle\int\limits_{\mathrm{T}_{\boldsymbol{\nu}}^s(\Gamma_\blacktriangle^0)} \int\limits_{\mathrm{T}_{\boldsymbol{\nu}}^s(\Gamma_\bullet^0)} \mathrm{G}^\Delta(\boldsymbol{x}, \boldsymbol{y}) \, \psi(\boldsymbol{y}) \, \phi(\boldsymbol{x}) \, d\mathrm{S}(\boldsymbol{y}) d\mathrm{S}(\boldsymbol{x}) \end{cases}
$$

$$
\mathrm{a}_{\mathrm{K}}^{\bullet, \blacktriangle}(s) : \begin{cases} H^{\frac{1}{2}}(\mathrm{T}_{\boldsymbol{\nu}}^s(\Gamma_\bullet^0)) \times H^{-\frac{1}{2}}(\mathrm{T}_{\boldsymbol{\nu}}^s(\Gamma_\blacktriangle^0)) \to \mathbb{R} \\ \mathrm{a}_{\mathrm{K}}^{\bullet, \blacktriangle}(s; g, \phi) := \displaystyle\int\limits_{\mathrm{T}_{\boldsymbol{\nu}}^s(\Gamma_\blacktriangle^0)} \int\limits_{\mathrm{T}_{\boldsymbol{\nu}}^s(\Gamma_\bullet^0)} \nabla_y \mathrm{G}^\Delta(\boldsymbol{x}, \boldsymbol{y}) \cdot \boldsymbol{n}_2^s(\boldsymbol{y}) \, g(\boldsymbol{y}) \, \phi(\boldsymbol{x}) \, d\mathrm{S}(\boldsymbol{y}) d\mathrm{S}(\boldsymbol{x}) \end{cases}
$$

$$
\mathrm{l}^{\bullet}(s) : \begin{cases} H^{\frac{1}{2}}(\mathrm{T}_{\boldsymbol{\nu}}^s(\Gamma_\bullet^0)) \times H^{-\frac{1}{2}}(\mathrm{T}_{\boldsymbol{\nu}}^s(\Gamma_\bullet^0)) \to \mathbb{R} \\ \mathrm{l}^{\bullet}(g, \phi) := \displaystyle\int\limits_{\mathrm{T}_{\boldsymbol{\nu}}^s(\Gamma_\bullet^0)} g(\boldsymbol{x}) \, \phi(\boldsymbol{x}) \, d\mathrm{S}(\boldsymbol{x}) \end{cases}
$$

$$
\mathrm{a}_{\mathrm{W}}^{\bullet, \blacktriangle}(s) : \begin{cases} H^{\frac{1}{2}}(\mathrm{T}_{\boldsymbol{\nu}}^s(\Gamma_\bullet^0)) \times H^{\frac{1}{2}}(\mathrm{T}_{\boldsymbol{\nu}}^s(\Gamma_\blacktriangle^0)) \to \mathbb{R} \\ \mathrm{a}_{\mathrm{W}}^{\bullet, \blacktriangle}(s; g, v) := \displaystyle\int\limits_{\mathrm{T}_{\boldsymbol{\nu}}^s(\Gamma_\blacktriangle^0)} \int\limits_{\mathrm{T}_{\boldsymbol{\nu}}^s(\Gamma_\bullet^0)} \mathrm{G}^\Delta(\boldsymbol{x}, \boldsymbol{y}) \, \frac{d}{dt} g(\boldsymbol{y}) \, \frac{d}{dt} v(\boldsymbol{x}) \, d\mathrm{S}(\boldsymbol{y}) d\mathrm{S}(\boldsymbol{x}) \quad (\text{2D}) \\ \mathrm{a}_{\mathrm{W}}^{\bullet, \blacktriangle}(s; g, v) := \displaystyle\int\limits_{\mathrm{T}_{\boldsymbol{\nu}}^s(\Gamma_\blacktriangle^0)} \int\limits_{\mathrm{T}_{\boldsymbol{\nu}}^s(\Gamma_\bullet^0)} \mathrm{G}^\Delta(\boldsymbol{x}, \boldsymbol{y}) \, \mathbf{curl}_\Gamma g(\boldsymbol{y}) \cdot \mathbf{curl}_\Gamma v(\boldsymbol{x}) \, d\mathrm{S}(\boldsymbol{y}) d\mathrm{S}(\boldsymbol{x}) \quad (\text{3D}) \end{cases}
$$

where $\bullet, \blacktriangle \in \{I, G\}$, $\Gamma_G^0 = \partial\Omega_0$ and Γ_I^0 is the reference interface. Note that in the new s-dependent expressions $\frac{d}{dt} g$ and $\boldsymbol{n}_2^s$ denote the arclength derivative and the unit normal vector field on the perturbed boundaries $\Gamma_\bullet^s := \mathrm{T}_{\boldsymbol{\nu}}^s(\Gamma_\bullet^0)$. This notation allows us to write the s dependent model problem in a similar compact way. We seek $\mathfrak{u}_s \in \tilde{H}^{\frac{1}{2}}(\Gamma_N^s)$, $\psi_s \in \tilde{H}^{-\frac{1}{2}}(\Gamma_D^s)$, $\mathfrak{u}_I^s \in H^{\frac{1}{2}}(\Gamma_I^s)$ and $\psi_I^s \in H^{-\frac{1}{2}}(\Gamma_I^s)$ such that

$$
\mathrm{a}_{\mathrm{W}}^{\mathrm{G,I}}(s; \mathfrak{u}_s, \mathfrak{v}_I) + (1 + \frac{\varepsilon_1}{\varepsilon_2}) \mathrm{a}_{\mathrm{W}}^{\mathrm{I,I}}(s; \mathfrak{u}_I^s, \mathfrak{v}_I) + \mathrm{a}_{\mathrm{K}}^{\mathrm{I,G}}(s; \mathfrak{v}_I, \psi_s) + 2\mathrm{a}_{\mathrm{K}}^{\mathrm{I,I}}(s; \mathfrak{v}_I, \psi_I^s)
$$

10

$$= -a_W^{G,I}(s; \mathfrak{g}_s', \mathfrak{v}_I) - a_K^{I,G}(s; \mathfrak{v}_I, \eta_s') \qquad \forall \mathfrak{v}_I \in H^{\frac{1}{2}}(\Gamma_I^s),$$

$$a_V^{G,I}(s; \psi_s, \phi_I) + (1 + \frac{\varepsilon_2}{\varepsilon_1}) a_V^{I,I}(s; \psi_I^s, \phi_I) - a_K^{G,I}(s; \mathfrak{u}_s, \phi_I) - 2a_K^{I,I}(s; \mathfrak{u}_I^s, \phi_I)$$

$$= -a_V^{G,I}(s; \eta_s', \phi_I) + a_K^{G,I}(s; \mathfrak{g}_s', \phi_I) \qquad \forall \phi_I \in H^{-\frac{1}{2}}(\Gamma_I^s),$$

$$a_V^{I,G}(s; \psi_I^s, \phi) + a_V^{G,G}(s; \psi_s, \phi) - a_K^{I,G}(s; \mathfrak{u}_I^s, \phi) - a_K^{G,G}(s; \mathfrak{u}_s, \phi)$$

$$= \frac{1}{2} l^G(s; \mathfrak{g}_s', \phi) - a_V^{G,G}(s; \eta_s', \phi) + a_K^{G,G}(s; \mathfrak{g}_s', \phi) \quad \forall \phi \in \tilde{H}^{-\frac{1}{2}}(\Gamma_D^s),$$

$$a_K^{I,G}(s; \mathfrak{u}_I^s, \mathfrak{v}) + a_K^{G,G}(s; \mathfrak{u}_s, \mathfrak{v}) + a_K^{G,G}(s; \mathfrak{v}, \psi_s) + a_K^{G,I}(\mathfrak{v}, \psi_I^s)$$

$$= \frac{1}{2} l^G(s; \mathfrak{v}, \eta_s') - a_K^{G,G}(s; \mathfrak{g}_s', \mathfrak{v}) - a_K^{G,G}(s; \mathfrak{v}, \eta_s') \quad \forall \mathfrak{v} \in \tilde{H}^{\frac{1}{2}}(\Gamma_N^s).$$

$$(20)$$

A possible way to choose these boundary conditions is by taking the trace of functions in volume, for example $\mathfrak{g}_s' := f|_{\partial \Omega_s} \in H^{\frac{1}{2}}(\partial \Omega_s)$ for some $f \in H^1(\mathbb{R}^2)$.

3.3 Transformation To Reference Domain

We begin by transforming the integrals back to the reference domain using the perturbation map. The objective is to write an equivalent problem to (20) on the reference configuration.

$$a_V^{\bullet, \blacktriangle}(s; \psi, \phi) = \int_{\Gamma_\blacktriangle^0} \int_{\Gamma_\bullet^0} G^\Delta(T_\nu^s(\boldsymbol{x}), T_\nu^s(\boldsymbol{y})) \, \psi(T_\nu^s(\boldsymbol{y})) \, \omega_s(\boldsymbol{y}) \, \phi(T_\nu^s(\boldsymbol{x})) \, \omega_s(\boldsymbol{x}) \, dS(\boldsymbol{y})dS(\boldsymbol{x}),$$

$$a_K^{\bullet, \blacktriangle}(s; g, \phi) = \int_{\Gamma_\blacktriangle^0} \int_{\Gamma_\bullet^0} \nabla_y G^\Delta(T_\nu^s(\boldsymbol{x}), T_\nu^s(\boldsymbol{y})) \cdot C(D\, T_\nu^s(\boldsymbol{y})) \boldsymbol{n}_2^0(\boldsymbol{y}) \, g(T_\nu^s(\boldsymbol{y})) \cdot$$

$$\phi(T_\nu^s(\boldsymbol{x})) \, \omega_s(\boldsymbol{x}) \, dS(\boldsymbol{y})dS(\boldsymbol{x}),$$

$$l^\bullet(s; g, \phi) = \int_{\Gamma_\bullet^0} g(T_\nu^s(\boldsymbol{x})) \, \phi(T_\nu^s(\boldsymbol{x})) \, \omega_s(\boldsymbol{x}) \, dS(\boldsymbol{x}),$$

$$(21)$$

$$a_W^{\bullet, \blacktriangle}(s; g, v) = \begin{cases} \int_{\Gamma_\blacktriangle^0} \int_{\Gamma_\bullet^0} G^\Delta(T_\nu^s(\boldsymbol{x}), T_\nu^s(\boldsymbol{y})) \, \frac{d}{dt} g(T_\nu^s(\boldsymbol{y})) \, \frac{d}{dt} v(T_\nu^s(\boldsymbol{x})) \cdot \\ \quad \omega_s(\boldsymbol{y}) \, \omega_s(\boldsymbol{x}) \, dS(\boldsymbol{y})dS(\boldsymbol{x}), & \text{(2D)} \\ \int_{\Gamma_\blacktriangle^0} \int_{\Gamma_\bullet^0} G^\Delta(T_\nu^s(\boldsymbol{x}), T_\nu^s(\boldsymbol{y})) \, \mathbf{curl}_\Gamma g(T_\nu^s(\boldsymbol{y})) \cdot \mathbf{curl}_\Gamma v(T_\nu^s(\boldsymbol{x})) \cdot \\ \quad \omega_s(\boldsymbol{y}) \, \omega_s(\boldsymbol{x}) \, dS(\boldsymbol{y})dS(\boldsymbol{x}), & \text{(3D)} \end{cases}$$

where $\boldsymbol{n}_2^0$ is the unit normal vector field on the reference boundary and $C(M)$ is the cofactor matrix of M. We have used the following identity for transformation of surface integrals [6, Ch. 9, Sec. 4.2, eq. 4.9], [19, Sect. 2.17] from $T_\nu^s(\Gamma)$ to Γ:

$$\int_{T_\nu^s(\Gamma)} f(\boldsymbol{x}') \, dS(\boldsymbol{x}') = \int_\Gamma (f \circ T_\nu^s)(\boldsymbol{x}) \, \omega_s(\boldsymbol{x}) \, dS(\boldsymbol{x}), \quad \omega_s(\boldsymbol{x}) := \left\| C(D\, T_\nu^s)(\boldsymbol{x}) \, \boldsymbol{n}^0(\boldsymbol{x}) \right\|, \; \boldsymbol{x} \in \Gamma,$$

and the identity for transformation of unit normal vector fields [6, Ch. 9, Thm. 4.4]

$$\boldsymbol{n}^s(T_\nu^s(\boldsymbol{x})) = \frac{C(D\, T_\nu^s(\boldsymbol{x})) \boldsymbol{n}^0(\boldsymbol{x})}{\| C(D\, T_\nu^s(\boldsymbol{x})) \boldsymbol{n}^0(\boldsymbol{x}) \|}, \; \boldsymbol{x} \in \Gamma,$$

11

3.4 Pullback Approach

The next step to achieve our objective of having an equivalent problem on the reference domain is the use of a pullback. Pullback allows us to get rid of the s-dependence of the function spaces. We use a pullback of surface charge densities for functions in $H^{-\frac{1}{2}}(\partial\Omega_s)$ and a pullback of potentials for functions in $H^{\frac{1}{2}}(\partial\Omega_s)$:

$$\hat{\psi} \in H^{-\frac{1}{2}}(\partial\Omega_0): \quad \hat{\psi} := (\psi \circ \mathrm{T}_{\boldsymbol{\nu}}^s)\,\omega_s, \quad \psi \in H^{-\frac{1}{2}}(\partial\Omega_s), \tag{22}$$

$$\hat{v} \in H^{\frac{1}{2}}(\partial\Omega_0): \quad \hat{v} := v \circ \mathrm{T}_{\boldsymbol{\nu}}^s, \qquad v \in H^{\frac{1}{2}}(\partial\Omega_s). \tag{23}$$

The pullback allows us to work with functions on the reference boundary which will be important in order to compute the energy shape derivative later. Since $\mathrm{T}_{\boldsymbol{\nu}}^s$ is a Lipschitz continuous mapping and $\omega_s \in L^\infty(\partial\Omega_s)$, the trace spaces are preserved under pullback. We also need additional transformation rules for the hypersingular bilinear form $a_{\mathrm{W}}^{\bullet,\blacktriangle}(s;g,v)$.

In 2D it involves the arclength derivative which transforms as

$$\frac{d}{dt}g(\mathrm{T}_{\boldsymbol{\nu}}^s(\boldsymbol{x})) = \lim_{||\boldsymbol{y}-\boldsymbol{x}||\to 0} \frac{g(\mathrm{T}_{\boldsymbol{\nu}}^s(\boldsymbol{x})) - g(\mathrm{T}_{\boldsymbol{\nu}}^s(\boldsymbol{y}))}{||\,\mathrm{T}_{\boldsymbol{\nu}}^s(\boldsymbol{x}) - \mathrm{T}_{\boldsymbol{\nu}}^s(\boldsymbol{y})||} = \lim_{||\boldsymbol{y}-\boldsymbol{x}||\to 0} \frac{g \circ \mathrm{T}_{\boldsymbol{\nu}}^s(\boldsymbol{x}) - g \circ \mathrm{T}_{\boldsymbol{\nu}}^s(\boldsymbol{y})}{\omega_s(\boldsymbol{x})||\boldsymbol{y}-\boldsymbol{x}||} = \frac{1}{\omega_s(\boldsymbol{x})}\frac{d\hat{g}}{d\hat{t}}(\boldsymbol{x}),$$

where $\frac{d\hat{g}}{d\hat{t}}$ is the arclength derivative on the reference boundary.

In 3D we have the surface curl operator. We begin by noting that $\mathbf{curl}_\Gamma u(\boldsymbol{x}) := \mathbf{grad}_\Gamma u(\boldsymbol{x}) \times \boldsymbol{n}(\boldsymbol{x}) = \nabla\tilde{u}(\boldsymbol{x}) \times \boldsymbol{n}(\boldsymbol{x})$, where $\tilde{u}: \mathbb{R}^3 \to \mathbb{R}$ is an extension of $u \in C^1(\Gamma)$ to a neighborhood of the surface Γ with an outward normal $\boldsymbol{n}(\boldsymbol{x})$. Using the transformation rules for the gradient and the normal we get

$$\mathbf{curl}_\Gamma u(\mathrm{T}_{\boldsymbol{\nu}}^s(\boldsymbol{x})) = \nabla\tilde{u}(\mathrm{T}_{\boldsymbol{\nu}}^s(\boldsymbol{x})) \times \boldsymbol{n}(\mathrm{T}_{\boldsymbol{\nu}}^s(\boldsymbol{x}))$$

$$= \mathrm{D}\,\mathrm{T}_{\boldsymbol{\nu}}^s(\boldsymbol{x})^{-T}(\nabla\tilde{u} \circ \mathrm{T}_{\boldsymbol{\nu}}^s)(\boldsymbol{x}) \times \frac{\mathrm{D}\,\mathrm{T}_{\boldsymbol{\nu}}^s(\boldsymbol{x})^{-T}\,\boldsymbol{n}_0(\boldsymbol{x})}{\|\mathrm{D}\,\mathrm{T}_{\boldsymbol{\nu}}^s(\boldsymbol{x})^{-T}\,\boldsymbol{n}_0(\boldsymbol{x})\|}$$

$$= \frac{\det(\mathrm{D}\,\mathrm{T}_{\boldsymbol{\nu}}^s(\boldsymbol{x})^{-T})\,\mathrm{D}\,\mathrm{T}_{\boldsymbol{\nu}}^s(\boldsymbol{x})}{\|\mathrm{D}\,\mathrm{T}_{\boldsymbol{\nu}}^s(\boldsymbol{x})^{-T}\,\boldsymbol{n}_0(\boldsymbol{x})\|}\big((\nabla\tilde{u} \circ \mathrm{T}_{\boldsymbol{\nu}}^s)(\boldsymbol{x}) \times \boldsymbol{n}_0(\boldsymbol{x})\big) = \frac{\mathrm{D}\,\mathrm{T}_{\boldsymbol{\nu}}^s(\boldsymbol{x})}{\omega_s(\boldsymbol{x})}(\mathrm{curl}_{\Gamma_0} u \circ \mathrm{T}_{\boldsymbol{\nu}}^s)(\boldsymbol{x}),$$

where we used the identity $(\mathbf{Ma}) \times (\mathbf{Mb}) = \det(\mathbf{M})\mathbf{M}^{-T}(\mathbf{a} \times \mathbf{b})$ for a regular matrix $\mathbf{M} \in \mathbb{R}^{3,3}$ and vectors $\mathbf{a}, \mathbf{b} \in \mathbb{R}^3$, and $\boldsymbol{n}_0(\boldsymbol{x})$ is the outward normal and $\mathbf{curl}_{\Gamma_0}$ is the surface curl on the reference boundary Γ_0.

Based on the pullbacks, we define (bi)linear forms on reference boundaries which look similar to (21) but include functions from spaces on the reference domain.

$$\hat{a}_V^{\bullet;\blacktriangle}(s;\hat{\psi},\hat{\phi}) := \int_{\Gamma_\blacktriangle^0}\int_{\Gamma_\bullet^0} \mathrm{G}^\Delta(\mathrm{T}_{\boldsymbol{\nu}}^s(\boldsymbol{x}),\mathrm{T}_{\boldsymbol{\nu}}^s(\boldsymbol{y}))\,\hat{\psi}(\boldsymbol{y})\,\hat{\phi}(\boldsymbol{x})\,d\mathrm{S}(\boldsymbol{y})d\mathrm{S}(\boldsymbol{x}),$$

$$\hat{a}_K^{\bullet;\blacktriangle}(s;\hat{g},\hat{\phi}) := \int_{\Gamma_\blacktriangle^0}\int_{\Gamma_\bullet^0} \nabla_y\mathrm{G}^\Delta(\mathrm{T}_{\boldsymbol{\nu}}^s(\boldsymbol{x}),\mathrm{T}_{\boldsymbol{\nu}}^s(\boldsymbol{y})) \cdot \mathrm{C}(\mathrm{D}\,\mathrm{T}_{\boldsymbol{\nu}}^s(\boldsymbol{y}))\boldsymbol{n}_2^0(\boldsymbol{y})\,\hat{g}(\boldsymbol{y})\,\hat{\phi}(\boldsymbol{x})\,d\mathrm{S}(\boldsymbol{y})d\mathrm{S}(\boldsymbol{x}),$$

$$\hat{l}^\bullet(s;\hat{g},\hat{\phi}) := \int_{\Gamma_\bullet^0} \hat{g}(\boldsymbol{x})\,\hat{\phi}(\boldsymbol{x})\,d\mathrm{S}(\boldsymbol{x}).$$

$$\hat{a}_W^{\bullet,\blacktriangle}(s;\hat{g},\hat{v}) := \begin{cases} \displaystyle\int_{\Gamma_\blacktriangle^0}\int_{\Gamma_\bullet^0} \mathrm{G}^\Delta(\mathrm{T}_{\boldsymbol{\nu}}^s(\boldsymbol{x}),\mathrm{T}_{\boldsymbol{\nu}}^s(\boldsymbol{y}))\,\frac{d}{d\hat{t}}\hat{g}(\boldsymbol{y})\,\frac{d}{d\hat{t}}\hat{v}(\boldsymbol{x})\,d\mathrm{S}(\boldsymbol{y})d\mathrm{S}(\boldsymbol{x}), & \text{(2D)} \\[2em] \displaystyle\int_{\Gamma_\blacktriangle^0}\int_{\Gamma_\bullet^0} \mathrm{G}^\Delta(\mathrm{T}_{\boldsymbol{\nu}}^s(\boldsymbol{x}),\mathrm{T}_{\boldsymbol{\nu}}^s(\boldsymbol{y}))\,\big(\mathrm{D}\,\mathrm{T}_{\boldsymbol{\nu}}^s(\boldsymbol{y})\,\mathbf{curl}_{\Gamma_0}\,\hat{g}(\boldsymbol{y})\big)\cdot \\[0.5em] \qquad\qquad \big(\mathrm{D}\,\mathrm{T}_{\boldsymbol{\nu}}^s(\boldsymbol{x})\,\mathbf{curl}_{\Gamma_0}\,\hat{v}(\boldsymbol{x})\big)\,d\mathrm{S}(\boldsymbol{y})d\mathrm{S}(\boldsymbol{x}) & \text{(3D)} \end{cases}$$

12

Using a similar procedure we can also get a transformed energy functional $\hat{J}$

$$\hat{J}(s; \hat{\mathfrak{u}}, \hat{\psi}) := \frac{\varepsilon_2}{2} \int\limits_{\partial\Omega_0} (\hat{\mathfrak{u}}(\boldsymbol{x}) + \hat{\mathfrak{g}}'_s(\boldsymbol{x})) \, (\hat{\eta}'_s(\boldsymbol{x}) + \hat{\psi}(\boldsymbol{x})) \, dS(\boldsymbol{x})$$

Finally our system of equations become: seek $\hat{\mathfrak{u}}_s \in \tilde{H}^{\frac{1}{2}}(\Gamma_N^0)$, $\hat{\psi}_s \in \tilde{H}^{-\frac{1}{2}}(\Gamma_D^0)$, $\hat{\mathfrak{u}}_I^s \in H^{\frac{1}{2}}(\Gamma_I^0)$ and $\hat{\psi}_I^s \in H^{-\frac{1}{2}}(\Gamma_I^0)$ such that

$$\hat{a}_W^{G,I}(s; \hat{\mathfrak{u}}_s, \hat{\mathfrak{v}}_I) + (1 + \frac{\varepsilon_1}{\varepsilon_2})\hat{a}_W^{I,I}(s; \hat{\mathfrak{u}}_I^s, \hat{\mathfrak{v}}_I) + \hat{a}_K^{I,G}(s; \hat{\mathfrak{v}}_I, \hat{\psi}_s) + 2\hat{a}_K^{I,I}(s; \hat{\mathfrak{v}}_I, \hat{\psi}_I^s)$$
$$= -\hat{a}_W^{G,I}(s; \hat{\mathfrak{g}}'_s, \hat{\mathfrak{v}}_I) - \hat{a}_K^{I,G}(s; \hat{\mathfrak{v}}_I, \hat{\eta}'_s) \qquad \forall \hat{\mathfrak{v}}_I \in H^{\frac{1}{2}}(\Gamma_I^0),$$
$$\hat{a}_V^{G,I}(s; \hat{\psi}_s, \hat{\phi}_I) + (1 + \frac{\varepsilon_2}{\varepsilon_1})\hat{a}_V^{I,I}(s; \hat{\psi}_I^s, \hat{\phi}_I) - \hat{a}_K^{G,I}(s; \hat{\mathfrak{u}}_s, \hat{\phi}_I) - 2\hat{a}_K^{I,I}(s; \hat{\mathfrak{u}}_I^s, \hat{\phi}_I)$$
$$= -\hat{a}_V^{G,I}(s; \hat{\eta}'_s, \hat{\phi}_I) + \hat{a}_K^{G,I}(s; \hat{\mathfrak{g}}'_s, \hat{\phi}_I) \qquad \forall \hat{\phi}_I \in H^{-\frac{1}{2}}(\Gamma_I^0),$$
$$\hat{a}_V^{I,G}(s; \hat{\psi}_I^s, \hat{\phi}) + \hat{a}_V^{G,G}(s; \hat{\psi}_s, \hat{\phi}) - \hat{a}_K^{I,G}(s; \hat{\mathfrak{u}}_I^s, \hat{\phi}) - \hat{a}_K^{G,G}(s; \hat{\mathfrak{u}}_s, \hat{\phi})$$
$$= \frac{1}{2} l^G(s; \hat{\mathfrak{g}}'_s, \hat{\phi}) - \hat{a}_V^{G,G}(s; \hat{\eta}'_s, \hat{\phi}) + \hat{a}_K^{G,G}(s; \hat{\mathfrak{g}}'_s, \hat{\phi}) \quad \forall \hat{\phi} \in \tilde{H}^{-\frac{1}{2}}(\Gamma_D^0),$$
$$\hat{a}_W^{I,G}(s; \hat{\mathfrak{u}}_I^s, \tilde{\mathfrak{v}}) + \hat{a}_W^{G,G}(s; \hat{\mathfrak{u}}_s, \hat{\mathfrak{v}}) + \hat{a}_K^{G,G}(s; \hat{\mathfrak{v}}, \hat{\psi}_s) + \hat{a}_K^{G,I}(s; \hat{\mathfrak{v}}, \hat{\psi}_I^s)$$
$$= \frac{1}{2} l^G(s; \hat{\mathfrak{v}}, \hat{\eta}'_s) - \hat{a}_W^{G,G}(s; \hat{\mathfrak{g}}'_s, \hat{\mathfrak{v}}) - \hat{a}_K^{G,G}(s; \hat{\mathfrak{v}}, \hat{\eta}'_s) \quad \forall \hat{\mathfrak{v}} \in \tilde{H}^{\frac{1}{2}}(\Gamma_N^0).$$
$$\tag{24}$$

At this point we make the assumption that $\boldsymbol{\nu}|_{\partial\Omega_0} \equiv 0$. Consequently the boundary $\partial\Omega_0$ does not change under the perturbation map, neither do the known traces on $\partial\Omega_0$. Exploting this we write $\hat{\eta}'_s = \eta'$ and $\hat{\mathfrak{g}}'_s = \mathfrak{g}'$ which will make the task of computing partial derivatives with respect to s easier in the next sub-section.

Introducing the notation $V := \tilde{H}^{-\frac{1}{2}}(\Gamma_D^0) \times \tilde{H}^{\frac{1}{2}}(\Gamma_N^0) \times H^{-\frac{1}{2}}(\Gamma_I^0) \times H^{\frac{1}{2}}(\Gamma_I^0)$, $\mathbf{X} := (\hat{\psi}, \hat{\mathfrak{u}}, \hat{\psi}_I, \hat{\mathfrak{u}}_I) \in V$, $\mathbf{X}_s := (\hat{\psi}_s, \hat{\mathfrak{u}}_s, \hat{\psi}_I^s, \hat{\mathfrak{u}}_I^s) \in V$ and $\mathbf{Y} := (\hat{\phi}, \hat{\mathfrak{v}}, \hat{\phi}_I, \hat{\mathfrak{v}}_I) \in V$, the system of equations in (24) can be written as: seek $\mathbf{X}_s \in V$ such that $A(s; \mathbf{X}_s, \mathbf{Y}) = L(s; \mathbf{Y}) \quad \forall \mathbf{Y} \in V$. The bilinear and linear forms A and L are given as

$$A : \mathbb{R} \times V \times V \to \mathbb{R}, \quad A(s; \mathbf{X}, \mathbf{Y}) :=$$
$$\hat{a}_W^{G,I}(s; \hat{\mathfrak{u}}, \hat{\mathfrak{v}}_I) + (1 + \frac{\varepsilon_1}{\varepsilon_2})\hat{a}_W^{I,I}(s; \hat{\mathfrak{u}}_I, \hat{\mathfrak{v}}_I) + \hat{a}_K^{I,G}(s; \hat{\mathfrak{v}}_I, \hat{\psi}) + 2\hat{a}_K^{I,I}(s; \hat{\mathfrak{v}}_I, \hat{\psi}_I) +$$
$$\hat{a}_V^{G,I}(s; \hat{\psi}, \hat{\phi}_I) + (1 + \frac{\varepsilon_2}{\varepsilon_1})\hat{a}_V^{I,I}(s; \hat{\psi}_I, \hat{\phi}_I) - \hat{a}_K^{G,I}(s; \hat{\mathfrak{u}}, \hat{\phi}_I) - 2\hat{a}_K^{I,I}(s; \hat{\mathfrak{u}}_I, \hat{\phi}_I) +$$
$$\hat{a}_V^{I,G}(s; \hat{\psi}_I, \hat{\phi}) + \hat{a}_V^{G,G}(s; \hat{\psi}, \hat{\phi}) - \hat{a}_K^{I,G}(s; \hat{\mathfrak{u}}_I, \hat{\phi}) - \hat{a}_K^{G,G}(s; \hat{\mathfrak{u}}, \hat{\phi}) +$$
$$\hat{a}_W^{I,G}(s; \hat{\mathfrak{u}}_I, \hat{\mathfrak{v}}) + \hat{a}_W^{G,G}(s; \hat{\mathfrak{u}}, \hat{\mathfrak{v}}) + \hat{a}_K^{G,G}(s; \hat{\mathfrak{v}}, \hat{\psi}) + \hat{a}_K^{G,I}(s; \hat{\mathfrak{v}}, \hat{\psi}_I)$$

$$L : \mathbb{R} \times V \to \mathbb{R}, \quad L(s; \mathbf{Y}) :=$$
$$- \hat{a}_W^{G,I}(s; \mathfrak{g}', \hat{\mathfrak{v}}_I) - \hat{a}_K^{I,G}(s; \hat{\mathfrak{v}}_I, \eta') - \hat{a}_V^{G,I}(s; \eta', \hat{\phi}_I) + \hat{a}_K^{G,I}(s; \mathfrak{g}', \hat{\phi}_I) +$$
$$\frac{1}{2}\hat{l}^G(s; \mathfrak{g}', \hat{\phi}) - \hat{a}_V^{G,G}(s; \eta', \hat{\phi}) + \hat{a}_K^{G,G}(s; \mathfrak{g}', \hat{\phi}) + \frac{1}{2}\hat{l}^G(s; \hat{\mathfrak{v}}, \eta') -$$
$$\hat{a}_W^{G,G}(s; \mathfrak{g}', \hat{\mathfrak{v}}) - \hat{a}_K^{G,G}(s; \hat{\mathfrak{v}}, \eta')$$

This formulation is equivalent to our s-dependent model problem as a solution of the original formulation (20) also solves this pulled back formulation by definition. Conversely, if $\hat{\mathfrak{u}}_s \in$

$\tilde{H}^{\frac{1}{2}}(\Gamma_N^0)$, $\hat{\psi}_s \in \tilde{H}^{-\frac{1}{2}}(\Gamma_D^0)$, $\hat{\mathfrak{u}}_I^s \in H^{\frac{1}{2}}(\Gamma_I^0)$ and $\hat{\psi}_I^s \in H^{-\frac{1}{2}}(\Gamma_I^0)$ solve (24) then using the fact that $\mathrm{T}_{\boldsymbol{\nu}}^s$ is a diffeomorphism and using the pullbacks, we recover the original formulation (20).

3.5   BIE Constrained Shape Derivative: Adjoint Method

While shape differentiating the field energy, we need to account for the constraint (24). We do this using the well-established adjoint approach [13, Sect. 1.6.4]. We start by defining the Lagrangian:

$$\mathcal{L} : \mathbb{R} \times V \times V \to \mathbb{R}, \quad \mathcal{L}(s; \mathbf{X}, \mathbf{Y}) := \mathrm{A}(s; \mathbf{X}, \mathbf{Y}) - \mathrm{L}(s; \mathbf{Y}) + \mathrm{J}(s; \mathbf{X}),$$

where

$$\mathrm{J} : \mathbb{R} \times V \to \mathbb{R}, \quad \mathrm{J}(s; \mathbf{X}) := \frac{\varepsilon_2}{2} \int_{\partial\Omega_0} (\hat{\mathfrak{u}}(\boldsymbol{x}) + \mathfrak{g}'(\boldsymbol{x})) \, (\eta'(\boldsymbol{x}) + \hat{\psi}(\boldsymbol{x})) \, d\mathrm{S}(\boldsymbol{x})$$

We recover the energy functional by plugging in the pulled back state solution into the Lagrangian.

$$\mathcal{L}(s; \mathbf{X}_s, \mathbf{Y}) = \mathrm{J}(s; X_s) = \mathcal{J}_F(s)$$

Using the adjoint solution $\mathbf{P}$, the shape derivative is given as:

$$\frac{d}{ds}\mathcal{J}_F(0) = \frac{\partial}{\partial s}\mathcal{L}(0; \mathbf{X}_0, \mathbf{P})$$

where the adjoint solution $\mathbf{P} := (\hat{\rho}, \hat{p}, \hat{\rho}_I, \hat{p}_I)$ solves the equation $\left\langle \frac{\partial}{\partial \mathbf{X}}\mathcal{L}(0; \mathbf{X}_0, \mathbf{P}); \mathbf{Z} \right\rangle = 0 \quad \forall \mathbf{Z} := (\beta, w, \beta_I, w_I) \in V$. Written out more explicitly, the adjoint equation is

$$\mathrm{A}(0; \mathbf{Z}, \mathbf{P}) = -\frac{\varepsilon_2}{2}\left(\hat{\mathrm{l}}^G(w, \eta' + \hat{\psi}_0) + \hat{\mathrm{l}}^G(\mathfrak{g}' + \hat{\mathfrak{u}}_0, \beta)\right) \quad \forall \mathbf{Z} \in V. \tag{25}$$

The adjoint equation contains a similar LHS to our state problem (24) and a modified RHS. The partial derivatives with respect to s are computed by differentiating with respect to s under the

14

integral

$$\frac{\partial}{\partial s}\hat{a}_{V}^{\bullet;\blacktriangle}(0;\hat{\psi},\hat{\phi}) = \int\limits_{\Gamma_{\blacktriangle}^{0}}\int\limits_{\Gamma_{\bullet}^{0}}(\nabla_{x}G^{\Delta}(\boldsymbol{x},\boldsymbol{y})\cdot\boldsymbol{\nu}(\boldsymbol{x}) + \nabla_{y}G^{\Delta}(\boldsymbol{x},\boldsymbol{y})\cdot\boldsymbol{\nu}(\boldsymbol{y}))\,\hat{\psi}(\boldsymbol{y})\,\hat{\phi}(\boldsymbol{x})\,dS(\boldsymbol{y})dS(\boldsymbol{x}),$$

$$\frac{\partial}{\partial s}\hat{a}_{K}^{\bullet;\blacktriangle}(0;\hat{g},\hat{\phi}) = \int\limits_{\Gamma_{\blacktriangle}^{0}}\int\limits_{\Gamma_{\bullet}^{0}}(\nabla_{x}(\nabla_{y}G^{\Delta}(\boldsymbol{x},\boldsymbol{y}))^{T}\cdot\boldsymbol{\nu}(\boldsymbol{x}) + \nabla_{y}(\nabla_{y}G^{\Delta}(\boldsymbol{x},\boldsymbol{y}))^{T}\cdot\boldsymbol{\nu}(\boldsymbol{y}))\cdot\boldsymbol{n}_{2}^{0}(\boldsymbol{y})\cdot$$

$$\hat{g}(\boldsymbol{y})\,\hat{\phi}(\boldsymbol{x})\,dS(\boldsymbol{y})dS(\boldsymbol{x}) +$$

$$\int\limits_{\Gamma_{\blacktriangle}^{0}}\int\limits_{\Gamma_{\bullet}^{0}}\nabla_{y}G^{\Delta}(\boldsymbol{x},\boldsymbol{y})\cdot(\nabla\cdot\boldsymbol{\nu}(\boldsymbol{y})\boldsymbol{n}_{2}^{0}(\boldsymbol{y}) - D\boldsymbol{\nu}^{T}(\boldsymbol{y})\boldsymbol{n}_{2}^{0}(\boldsymbol{y}))\cdot$$

$$\hat{g}(\boldsymbol{y})\,\hat{\phi}(\boldsymbol{x})\,dS(\boldsymbol{y})dS(\boldsymbol{x}),$$

$$\frac{\partial}{\partial s}\hat{l}^{\bullet}(0;\hat{g},\hat{\phi}) = 0, \tag{26}$$

$$\frac{\partial}{\partial s}\hat{a}_{W}^{\bullet;\blacktriangle}(0;\hat{g},\hat{v}) = \begin{cases} \int\limits_{\Gamma_{\blacktriangle}^{0}}\int\limits_{\Gamma_{\bullet}^{0}}(\nabla_{x}G^{\Delta}(\boldsymbol{x},\boldsymbol{y})\cdot\boldsymbol{\nu}(\boldsymbol{x}) + \nabla_{y}G^{\Delta}(\boldsymbol{x},\boldsymbol{y})\cdot\boldsymbol{\nu}(\boldsymbol{y}))\cdot \\ \qquad\frac{d}{d\hat{t}}\hat{g}(\boldsymbol{y})\,\frac{d}{d\hat{t}}\hat{v}(\boldsymbol{x})\,dS(\boldsymbol{y})dS(\boldsymbol{x}), \qquad\qquad\text{(2D)} \\ \int\limits_{\Gamma_{\blacktriangle}^{0}}\int\limits_{\Gamma_{\bullet}^{0}}(\nabla_{x}G^{\Delta}(\boldsymbol{x},\boldsymbol{y})\cdot\boldsymbol{\nu}(\boldsymbol{x}) + \nabla_{y}G^{\Delta}(\boldsymbol{x},\boldsymbol{y})\cdot\boldsymbol{\nu}(\boldsymbol{y}))\cdot \\ \qquad\mathbf{curl}_{\Gamma}\,\hat{g}(\boldsymbol{y})\cdot\mathbf{curl}_{\Gamma}\,\hat{v}(\boldsymbol{x})\,dS(\boldsymbol{y})dS(\boldsymbol{x}) + \qquad\text{(3D)} \\ \int\limits_{\Gamma_{\blacktriangle}^{0}}\int\limits_{\Gamma_{\bullet}^{0}}G^{\Delta}(\boldsymbol{x},\boldsymbol{y})\left((D\boldsymbol{\nu}(\boldsymbol{y})\,\mathbf{curl}_{\Gamma}\,\hat{g}(\boldsymbol{y}))\cdot\mathbf{curl}_{\Gamma}\,\hat{v}(\boldsymbol{x}) + \right. \\ \qquad\left.\mathbf{curl}_{\Gamma}\,\hat{g}(\boldsymbol{y})\cdot(D\boldsymbol{\nu}(\boldsymbol{x})\,\mathbf{curl}_{\Gamma}\,\hat{v}(\boldsymbol{x}))\right)\,dS(\boldsymbol{y})dS(\boldsymbol{x}), \end{cases}$$

where we have used the identities [19, Sect. 2.13]

$$\frac{\partial}{\partial s}f\circ T_{\boldsymbol{\nu}}^{s}\,|_{s=0} = \nabla f\cdot\boldsymbol{\nu}, \qquad \frac{\partial}{\partial s}\,C(D\,T_{\boldsymbol{\nu}}^{s})|_{s=0} = \nabla\cdot\boldsymbol{\nu}\,\mathbf{I}_{d} - (D\boldsymbol{\nu})^{T}.$$

The energy shape derivative is obtained by combining these partial derivatives

$$\frac{d}{ds}\mathcal{J}_{F}(0)[\mathbf{X}_{0},\mathbf{P}] = \frac{\partial}{\partial s}\mathcal{L}(0;\mathbf{X}_{0},\mathbf{P}) = \frac{\partial}{\partial s}A(0;\mathbf{X}_{0},\mathbf{P}) - \frac{\partial}{\partial s}L(0;\mathbf{P}) + \frac{\partial}{\partial s}J(0;\mathbf{X}_{0}) =$$

$$\frac{\partial}{\partial s}\hat{a}_{W}^{G,I}(0;\hat{u}_{0},\hat{p}_{I}) + (1+\frac{\varepsilon_{1}}{\varepsilon_{2}})\frac{\partial}{\partial s}\hat{a}_{W}^{I,I}(0;\hat{u}_{I}^{0},\hat{p}_{I}) + \frac{\partial}{\partial s}\hat{a}_{K}^{I,G}(0;\hat{p}_{I},\hat{\psi}_{0}) + 2\frac{\partial}{\partial s}\hat{a}_{K}^{I,I}(0;\hat{p}_{I},\hat{\psi}_{I}^{0})$$

$$+ \frac{\partial}{\partial s}\hat{a}_{V}^{G,I}(0;\hat{\psi}_{0},\hat{\rho}_{I}) + (1+\frac{\varepsilon_{2}}{\varepsilon_{1}})\frac{\partial}{\partial s}\hat{a}_{V}^{I,I}(0;\hat{\psi}_{I}^{0},\hat{\rho}_{I}) - \frac{\partial}{\partial s}\hat{a}_{K}^{G,I}(0;\hat{u}_{0},\hat{\rho}_{I}) - 2\frac{\partial}{\partial s}\hat{a}_{K}^{I,I}(0;\hat{u}_{I}^{0},\hat{\rho}_{I})$$

$$+ \frac{\partial}{\partial s}\hat{a}_{V}^{I,G}(0;\hat{\psi}_{I}^{0},\hat{\rho}) + \frac{\partial}{\partial s}\hat{a}_{V}^{G,G}(0;\hat{\psi}_{0},\hat{\rho}) - \frac{\partial}{\partial s}\hat{a}_{K}^{I,G}(0;\hat{u}_{I}^{0},\hat{\rho}) - \frac{\partial}{\partial s}\hat{a}_{K}^{G,G}(0;\hat{u}_{0},\hat{\rho})$$

$$+ \frac{\partial}{\partial s}\hat{a}_{W}^{I,G}(0;\hat{u}_{I}^{0},\hat{p}) + \frac{\partial}{\partial s}\hat{a}_{W}^{G,G}(0;\hat{u}_{0},\hat{p}) + \frac{\partial}{\partial s}\hat{a}_{K}^{G,G}(0;\hat{p},\hat{\psi}_{0}) + \frac{\partial}{\partial s}\hat{a}_{K}^{G,I}(0;\hat{p},\hat{\psi}_{I}^{0}) \tag{27}$$

$$+ \frac{\partial}{\partial s}\hat{a}_{W}^{G,I}(0;\mathfrak{g}',\hat{p}_{I}) + \frac{\partial}{\partial s}\hat{a}_{K}^{I,G}(0;\hat{p}_{I},\eta') + \frac{\partial}{\partial s}\hat{a}_{V}^{G,I}(0;\eta',\hat{\rho}_{I}) - \frac{\partial}{\partial s}\hat{a}_{K}^{G,I}(0;\mathfrak{g}',\hat{\rho}_{I})$$

$$- \frac{1}{2}\frac{\partial}{\partial s}\hat{l}^{G}(0;\mathfrak{g}',\hat{\rho}) + \frac{\partial}{\partial s}\hat{a}_{V}^{G,G}(0;\eta',\hat{\rho}) - \frac{\partial}{\partial s}\hat{a}_{K}^{G,G}(0;\mathfrak{g}',\hat{\rho}) - \frac{1}{2}\frac{\partial}{\partial s}\hat{l}^{G}(0;\hat{p},\eta')$$

$$+ \frac{\partial}{\partial s}\hat{a}_{W}^{G,G}(0;\mathfrak{g}',\hat{p}) + \frac{\partial}{\partial s}\hat{a}_{K}^{G,G}(0;\hat{p},\eta'),$$

15

because $\frac{\partial}{\partial s}\mathrm{J}(0;\mathbf{X}_0) = 0$. Now we will study the properties of the shape derivative expression.

3.6 Properties of Shape Derivative Formula

We saw in the previous sub-section that the shape derivative formula is a sum of double integrals of the partial derivatives $\frac{\partial}{\partial s}\hat{\mathrm{a}}_{\mathrm{V}}^{\bullet,\blacktriangle}(0;\hat{\psi},\hat{\phi})$, $\frac{\partial}{\partial s}\hat{\mathrm{a}}_{\mathrm{K}}^{\bullet,\blacktriangle}(0;\hat{g},\hat{\phi})$ and $\frac{\partial}{\partial s}\hat{\mathrm{a}}_{\mathrm{W}}^{\bullet,\blacktriangle}(0;\hat{g},\hat{v})$ with the state and adjoint solutions plugged in. In this sub-section we will discuss the singularities of the kernels in these integrals which will determine the properties of these expressions. It is to be noted that when $\bullet \neq \blacktriangle$, the integrals are well defined as the singularity is never encountered in the double integral. So we will focus on the case $\bullet = \blacktriangle$ and write Γ instead of Γ_*. For the analysis we assume $\boldsymbol{\nu} \in (C_0^\infty(\Omega))^d$ and $\mathfrak{g}' \in C^\infty(\partial\Omega)$.

Next, we focus on the terms $\frac{\partial \hat{\mathrm{a}}_{\mathrm{V}}}{\partial s}$ and $\frac{\partial \hat{\mathrm{a}}_{\mathrm{W}}}{\partial s}$ to demonstrate the analysis techniques. A similar analysis for $\frac{\partial \hat{\mathrm{a}}_{\mathrm{K}}}{\partial s}$ can be found in [17, Sec. 4.4]. Using the expression for the fundamental solution, we obtain its gradient:

$$\nabla_y \mathrm{G}^\Delta(\boldsymbol{x},\boldsymbol{y}) = \frac{1}{2^{d-1}\pi}\frac{\boldsymbol{x}-\boldsymbol{y}}{\|\boldsymbol{x}-\boldsymbol{y}\|^d}, \quad d = 2,3.$$

The boundary integral operator T_{V} at the core of the expressions for $\frac{\partial \hat{\mathrm{a}}_{\mathrm{V}}}{\partial s}$ and $\frac{\partial \hat{\mathrm{a}}_{\mathrm{W}}}{\partial s}$ is

$$\mathrm{T}_{\mathrm{V}}\,\psi(\boldsymbol{x}) := -\frac{1}{2^{d-1}\pi}\int_\Gamma \frac{\boldsymbol{x}-\boldsymbol{y}}{\|\boldsymbol{x}-\boldsymbol{y}\|^d}\cdot\big(\boldsymbol{\nu}(\boldsymbol{x})-\boldsymbol{\nu}(\boldsymbol{y})\big)\,\psi(\boldsymbol{y})\,d\mathrm{S}(\boldsymbol{y}), \quad \boldsymbol{x}\in\Gamma \tag{28}$$

$$= -\frac{1}{2^{d-1}\pi}\int_\Gamma K_{\mathrm{V}}(\boldsymbol{x},\boldsymbol{x}-\boldsymbol{y})\,\psi(\boldsymbol{y})\,d\mathrm{S}(\boldsymbol{y}), \quad K_{\mathrm{V}}(\boldsymbol{x},\boldsymbol{z}) := \frac{\boldsymbol{z}}{\|\boldsymbol{z}\|^d}\cdot\big(\boldsymbol{\nu}(\boldsymbol{x})-\boldsymbol{\nu}(\boldsymbol{x}-\boldsymbol{z})\big).$$

Using the assumption on the velocity field $\boldsymbol{\nu}$, we can do a local Taylor expansion

$$\boldsymbol{\nu}(\boldsymbol{x})-\boldsymbol{\nu}(\boldsymbol{x}-\boldsymbol{z}) = \mathrm{D}\boldsymbol{\nu}(\boldsymbol{x})\boldsymbol{z} - \frac{1}{2}\mathrm{D}^2\boldsymbol{\nu}(\boldsymbol{x})(\boldsymbol{z},\boldsymbol{z}) + O(\|\boldsymbol{z}\|^3) \quad \text{for } \boldsymbol{z}\to 0,$$

which gives us

$$K_{\mathrm{V}}(\boldsymbol{x},\boldsymbol{z}) = K_{\mathrm{V}}^1(\boldsymbol{x},\boldsymbol{z}) + K_{\mathrm{V}}^2(\boldsymbol{x},\boldsymbol{z}), \quad K_{\mathrm{V}}^1(\boldsymbol{x},\boldsymbol{z}) := \frac{\boldsymbol{z}^T\mathrm{D}\boldsymbol{\nu}(\boldsymbol{x})\boldsymbol{z}}{\|\boldsymbol{z}\|^d}.$$

For $d = 2$ we observe that $K_{\mathrm{V}}^1(\boldsymbol{x},\boldsymbol{z})$ is a homogeneous kernel of class -1 as its first order derivatives in $\boldsymbol{z}$ are homogeneous with degree $-1 = -(d-1)$ and are odd. We also observe that $\boldsymbol{z} \mapsto K_{\mathrm{V}}^2(\boldsymbol{x},\boldsymbol{z}) \in W^{1,\infty}(\mathbb{R}^2)$ for all $\boldsymbol{x}\in\Omega$. Finally the assumptions on $\boldsymbol{\nu}$ give us regularity of $\boldsymbol{x} \mapsto K_{\mathrm{V}}(\boldsymbol{x},\boldsymbol{z})$. Thus $K_{\mathrm{V}}(\boldsymbol{x},\boldsymbol{z})$ is a pseudo-homogeneous kernel of class -1 according to the definition in [16, Sec. 4.3.3].

For $d = 3$ we first redefine the notations as

$$K_{\mathrm{V}}(\boldsymbol{x},\boldsymbol{z}) = K_{\mathrm{V}}^1(\boldsymbol{x},\boldsymbol{z}) + K_{\mathrm{V}}^2(\boldsymbol{x},\boldsymbol{z}) + K_{\mathrm{V}}^3(\boldsymbol{x},\boldsymbol{z}),$$

$$K_{\mathrm{V}}^1(\boldsymbol{x},\boldsymbol{z}) := \frac{\boldsymbol{z}^T\mathrm{D}\boldsymbol{\nu}(\boldsymbol{x})\boldsymbol{z}}{\|\boldsymbol{z}\|^d}, \quad K_{\mathrm{V}}^2(\boldsymbol{x},\boldsymbol{z}) := \frac{1}{2}\frac{\boldsymbol{z}^T\mathrm{D}^2\boldsymbol{\nu}(\boldsymbol{x})(\boldsymbol{z},\boldsymbol{z})}{\|\boldsymbol{z}\|^d}.$$

and see that the first order derivatives of $\boldsymbol{z} \mapsto K_{\mathrm{V}}^1(\boldsymbol{x},\boldsymbol{z})$ are homogeneous with degree $-2 = -(d-1)$ and are odd, making it pseudo homogeneous of class -1. The same holds true for the second order derivatives of $\boldsymbol{z} \mapsto K_{\mathrm{V}}^2(\boldsymbol{x},\boldsymbol{z})$ which makes it of class -2. The rest of the terms

16

encapsulated in $\boldsymbol{z} \mapsto K_{\mathrm{V}}^3(\boldsymbol{x}, \boldsymbol{z})$ belong to $W^{1,\infty}(\mathbb{R}^3)$. Using regularity of $\boldsymbol{\nu}$ we conclude that $K_{\mathrm{V}}(\boldsymbol{x}, \boldsymbol{z})$ is pseudo-homogeneous of class -1.

The pseudo-homogeneity discussed is enough to invoke [16, Thm. 4.3.2]. Combining it with results from [8, Sec. 1.3] on scales of Sobolev spaces $H^s(\Gamma)$ supported on boundaries of class $C^{r,1}, r \in \mathbb{N}_0$ [8, Def. 1.2.1.1], we get the mapping properties which are summarized next.

- Under the assumption on $\boldsymbol{\nu}$ and for Γ of class $C^{r,1}$, the boundary integral operator T_{V} from (3.6) is a bounded operator $H^{l-\frac{1}{2}}(\Gamma) \to H^{l+\frac{1}{2}}(\Gamma)$ for all $r - \frac{1}{2} \leq l \leq r + \frac{1}{2}$. By duality we have that $\frac{\partial \hat{\mathrm{a}}_{\mathrm{V}}}{\partial s}$ is a continuous mapping, $\frac{\partial \hat{\mathrm{a}}_{\mathrm{V}}}{\partial s} : H^{l-\frac{1}{2}}(\Gamma) \times H^{-l-\frac{1}{2}}(\Gamma) \to \mathbb{R}$.

- In 2D $\frac{\partial \hat{\mathrm{a}}_{\mathrm{W}}}{\partial s}$ contains one double integral which features the same pseudo-homogeneous kernel of class -1 as in $\frac{\partial \hat{\mathrm{a}}_{\mathrm{V}}}{\partial s}$. Using integration by parts $\frac{\partial \hat{\mathrm{a}}_{\mathrm{W}}}{\partial s}(0; u, v) = \left\langle v, \frac{d}{dt} \circ \mathrm{T}_{\mathrm{V}} \circ \frac{d}{dt}(u) \right\rangle_{L^2(\Gamma)}$. Since $\mathrm{T}_{\mathrm{V}} : H^l(\Gamma) \to H^{l+1}(\Gamma), -r - 1 \leq l \leq r$, we have $\frac{d}{dt} \circ \mathrm{T}_{\mathrm{V}} \circ \frac{d}{dt} : H^{l+1}(\Gamma) \to H^l(\Gamma)$ which yields that $\frac{\partial \hat{\mathrm{a}}_{\mathrm{W}}}{\partial s} : H^{l+1}(\Gamma) \times H^{-l}(\Gamma) \to \mathbb{R}$ is a continuous map.

- In 3D $\frac{\partial \hat{\mathrm{a}}_{\mathrm{W}}}{\partial s}$ contains two integrals with different kernels as seen in (26). The second integral is just the bilinear form for the Hypersingular BIO which is a continuous map $H^{l+1}(\Gamma) \times H^{-l}(\Gamma) \to \mathbb{R}$ for $-r - 1 \leq l \leq r$. We get the same mapping property for the first integral which features the pseudo-homogeneous kernel of class -1 from eq. (3.6), as seen in $\frac{\partial \hat{\mathrm{a}}_{\mathrm{V}}}{\partial s}$. Thus we find that $\frac{\partial \hat{\mathrm{a}}_{\mathrm{W}}}{\partial s} : H^{l+1}(\Gamma) \times H^{-l}(\Gamma) \to \mathbb{R}$ is a continuous map in 3D.

- For detailed analysis of $\frac{\partial \hat{\mathrm{a}}_{\mathrm{K}}}{\partial s}$ we refer to [17, Sec. 4.4] and simply mention the mapping property, $\frac{\partial \hat{\mathrm{a}}_{\mathrm{K}}}{\partial s} : H^l(\Gamma) \times H^{-l}(\Gamma) \to \mathbb{R}$ for Γ of class $C^{r,1}$, where $-r - 1 \leq l \leq r + 1$.

Summarizing the results we find that the shape derivative formula (27) is continuous on the energy trace spaces which also implies that it is C^∞-smooth, which enables its Galerkin approximation to enjoy superconvergence [17, Prop. 1.2].

4 Numerical Experiments in 2D

This section is focused on demonstrating the numerical efficacy of the new shape derivative formula (27) by using it to compute forces and torques, and comparing it with the interface-based methods introduced earlier in Section 2.3. For the sake of completeness, we will also show a comparison with a volume-based formula and FEM.

4.1 Implementation

The BEM solution for both state and adjoint problem is computed using 2DParametricBEM, a C++ library for BEM in 2D which uses exact parametrization for the boundaries. It evaluates the integrals with weakly singular kernels, like that of Single and Double layer potential, using log weighted Gauss quadrature (order 16) and regularization by transformation to polar coordinates [9, Section 9.4.5]. The state and adjoint solutions are evaluated using lowest order BEM spaces $S_0^{-1}(\partial \Omega_h)$ and $S_1^0(\partial \Omega_h)$ on a quasi-uniform sequence of mesh partitions of $\partial \Omega_2$ with decreasing meshwidth h. In the implementation, the extended trace $\mathfrak{g}'$ is constructed using a smooth extension of $\mathfrak{g}$ by zero to $\partial \Omega$, which on the discrete level can be implemented by using zero coefficients for $\mathfrak{g}_h' \in S_1^0(\mathcal{M}_h)$ on mesh elements corresponding to Γ_N. The extension of $\eta \equiv 0$ to η' is trivial.

The shape derivative formula (27) is also implemented in 2DParametricBEM using similar techniques to evaluate integrals with weakly singular kernels. For implementation we assume

that the perturbation field $\boldsymbol{\nu}$ is available in a functional form along with its first and second derivatives. Smooth integrals are simply evaluated using Gauss quadrature of order 16.

For comparison with the volume formula we use a FEM implementation[4] done using LehrFEM++. The potential solution u is evaluated directly inside the volume using $P1$ finite elements on a quasi-uniform sequence of triangular meshes Ω_h of Ω with decreasing mesh size h. Since the mesh is not parametric for FEM computations, a polygonal approximation of smooth curved boundaries is used.

4.2 Force Computation

For computing forces using the shape derivative formula, we use specific vector fields. The cartesian components of the net force $\mathbf{F} = (F_1, F_2, ..., F_d) \in \mathbb{R}^d$ acting on the interface Γ_I can be computed using vector fields parallel to the coordinate axis:

$$F_k = \frac{d\mathcal{J}_F}{d\Omega}(\Omega; \{\boldsymbol{x} \to \boldsymbol{e}_k \xi(\boldsymbol{x})\}),$$

where $\xi \in C_0^\infty(\Omega)$ and $\xi \equiv 1$ in a neighborhood of Γ_I. This makes the computations simpler as we can assume the first and second derivatives of the perturbation field to be zero in a neighborhood around Γ_I.

The force evaluated using the above recipe is compared to the interface based formula from (15), which is evaluated using the BEM solution and the trace of the FEM solution. For the sake of completeness we also do a comparison with the volume based "egg-shell" formula [10],[11],[15] which is computed by plugging the FEM solution into

$$\mathbf{F} = -\int_\Omega \varepsilon(\boldsymbol{x}) \left(\nabla u(\boldsymbol{x}) \left(\nabla u(\boldsymbol{x}) \cdot \nabla w(\boldsymbol{x}) \right) - \frac{1}{2} \|\nabla u(\boldsymbol{x})\|^2 \nabla w(\boldsymbol{x}) \right) d\boldsymbol{x}, \tag{29}$$

where $w \in W^{1,\infty}(\Omega)$ with $w|_{\Gamma_I} \equiv 1$ and $w|_{\partial\Omega} \equiv 0$. We perform numerical computations on two domains

- A square shaped $\Omega := (-2, 2)^2$ and a smooth kite-shaped Ω_1 given by the parametrization

$$\gamma : [0, 2\pi] \to \mathbb{R}^2, \ t \mapsto \begin{bmatrix} 0.3 + 0.5 \ \cos(t) + 0.1625 \ \cos(2t) \\ 0.5 + 0.35 \ \sin(t) \end{bmatrix}.$$

- A square shaped $\Omega := (-2, 2)^2$ and a square-shaped $\Omega_1 := (0, 1)^2$

The coarsest volume meshes can be seen in Figure 2 for both geometries. The Dirichlet boundary conditions in both cases are given as $\mathfrak{g}(-2, y) = 4, \mathfrak{g}(2, y) = 0, \ y \in [-2, 2]$ and the Neumann data $\eta = 0$. For the volume based formula (29), we use the cut-off function

$$w(\boldsymbol{x}) := \begin{cases} 1 & \text{for } \|\boldsymbol{x}\| < 1.4 \\ \cos^2(\frac{\|\boldsymbol{x}\| - 1.4}{0.5} \frac{\pi}{2}) & \text{for } 1.4 \leq \|\boldsymbol{x}\| \leq 1.9 \\ 0 & \text{for } \|\boldsymbol{x}\| > 1.9 \end{cases}$$

The reference values are computed using the shape derivative formula at a refinement level of 4728 panels for the kite-shaped Ω_1 and 5120 panels for the square-shaped Ω_1. Figure 3 shows the convergence plots for relative error of the computed force vs meshwidth h for both domains.

From the plots we can immediately see that the shape derivative formula outperforms other methods in terms of absolute accuracy as well as the asymptotic convergence rate, which are tabulated in Table 1. The worst formula in terms of performance is the interface-based formula from (15).
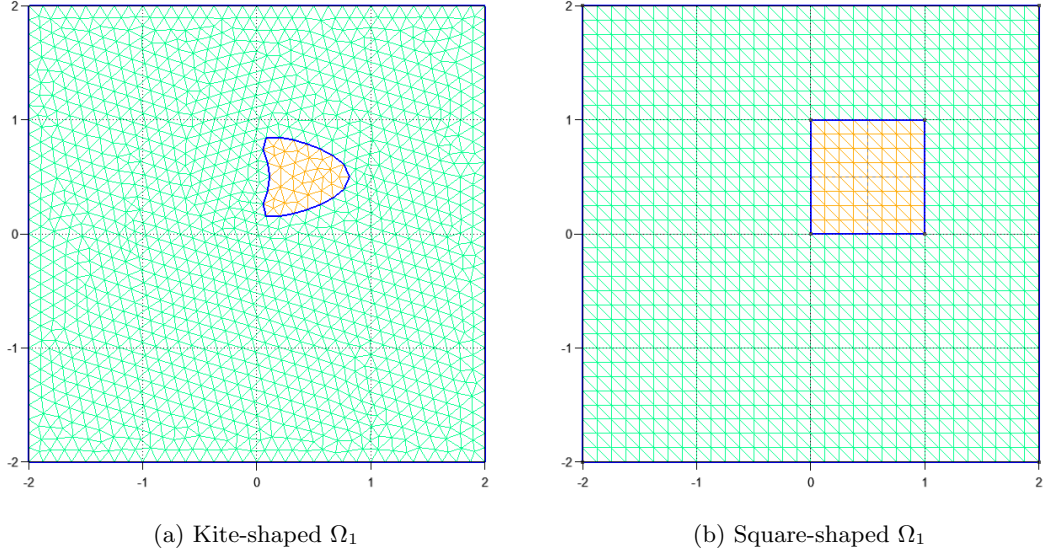
---

[4]Code is available at https://github.com/gninr/FCSCD.git

(a) Kite-shaped Ω_1

(b) Square-shaped Ω_1

Figure 2: Geometries for the numerical experiments

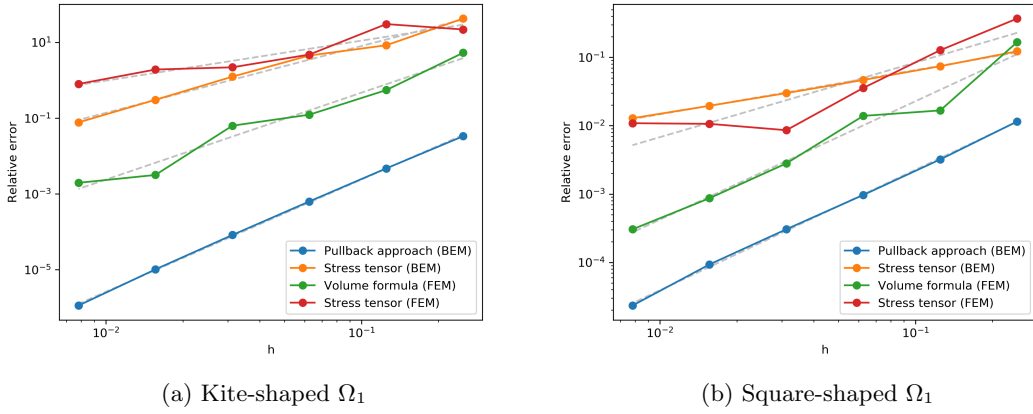
(a) Kite-shaped Ω_1

(b) Square-shaped Ω_1

Figure 3: Error of total forces as a function of the meshwidth h. Dashed lines represent the linear regression fits.

Table 1: Asymptotic rate of algebraic convergence

Method	Kite-shaped Ω_1	Square-shaped Ω_1
Pullback approach (BEM)	2.96	1.76
Stress tensor (BEM)	1.76	0.648
Volume formula (FEM)	2.29	1.73
Stress tensor (FEM)	1.06	1.09

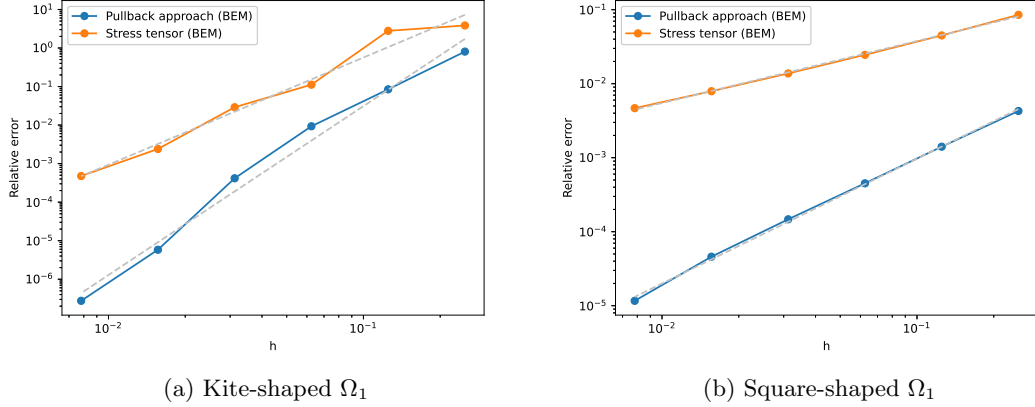(a) Kite-shaped Ω_1 (b) Square-shaped Ω_1

Figure 4: Error of net torque as a function of the meshwidth h. Dashed lines represent the linear regression fits.

4.3 Torque Computation

For computing the net torque about a point $\boldsymbol{c} \in \mathbb{R}^2$ using the shape derivative, we use a rotational field around the point $\boldsymbol{c}$. The net torque on Ω_1 is given as

$$T = \frac{d\mathcal{J}_F}{d\Omega}(\Omega; \{\boldsymbol{x} \to (\boldsymbol{x} - \boldsymbol{c})^{\perp} \xi(\boldsymbol{x})\}),$$

where $\xi \in C_0^{\infty}(\Omega)$ and $\xi \equiv 1$ in a neighborhood of Γ_I. This will be compared to torque computed using the Maxwell stress tensor formula. We know from Section 2.4 that the surface force density at the interface Γ_I is $[\mathbf{T}(u)] \cdot \boldsymbol{n}_1$. Using this we can compute torque on an infinitesimal section of the boundary and integrate it to get the net torque:

$$T = \int_{\Gamma_I} \det \left[\boldsymbol{x} - \boldsymbol{c}, \ [\mathbf{T}(u)(\boldsymbol{x})] \, \boldsymbol{n}(\boldsymbol{x}) \right] \ d\mathrm{S}(\boldsymbol{x}).$$

We use the determinant instead of a cross product which is used to define the torque. The reason for that is the 2D experimental setting. The torque can be evaluated using the cross product after extending the 2 dimensional vectors in our expression with a zero to make them a 3D vector. Numerical computations are done in the same experimental setting introduced in the previous subsection. As reference solution we use the torque evaluated using the shape derivative formula at a refinement level of 4728 panels for the kite-shaped Ω_1 and 5120 panels for square-shaped Ω_1. Figure 4 shows the plot of relative error in the computed torque vs the meshwidth h for both domains. The asymptotic convergence rates are given in Table 2.

Table 2: Asymptotic rate of algebraic convergence

Method	Kite-shaped Ω_1	Square-shaped Ω_1
Pullback approach (BEM)	4.38	1.69
Stress tensor (BEM)	2.78	0.84

20

5 Conclusion

Based on the virtual work principle and harnessing shape calculus we derived a new way for computing electrostatic forces on interfaces between homogeneous dielectric media. Our approach is compatible with the boundary element method in that it entirely relies on approximations of Dirichlet and Neumann traces on the interface and special boundary integral operators. Most importantly, the resulting expressions for the forces given in (27) are continuous functionals on energy trace spaces, which paves the way for superconvergence when they are used in the context with Galerkin approximation. In numerical experiments we have seen that this effect provides remarkably fast convergence and high accuracy of the computed forces. In this respect our new approach is clearly the best way to determine electrostatic forces in BEM-based simulations.

The use of the new formulas carries a price tag: It entails solving another discrete boundary integral equation, the adjoint problem, and the evaluating a number of integral operators with singular kernels. Fortunately, these operators are structurally similar to the standard integral operators and, therefore, amenable to the same regularizing quadrature schemes and compression techniques. This makes possible the reuse of existing algorithms and the data structures set up for compressing the regular discrete boundary integral operators can reused also for those occurring in the new formula (27).

References

[1] A. Bossavit. Forces in magnetostatics and their computation. *Journal of Applied Physics*, 67(9):5812–5814, 1990.

[2] Anthony Carpentier, Nicolas Galopin, Olivier Chadebec, Gérard Meunier, and Christophe Guérin. Application of the virtual work principle to compute magnetic forces with a volume integral method. *International Journal of Numerical Modelling: Electronic Networks, Devices and Fields*, 27(3):418–432, 2014.

[3] X. Claeys, R. Hiptmair, C. Jerez-Hanckes, and S. Pintarelli. Novel multi-trace boundary integral equations for transmission boundary value problems. In A.S. Fokas and B. Pelloni, editors, *Unified Transform for Boundary Value Problems: Applications and Advances*, pages 227–258. SIAM, Philadelphia, 2014.

[4] J.L. Coulomb. A methodology for the determination of global electromechanical quantities from a finite element analysis and its application to the evaluation of magnetic forces, torques and stiffness. *IEEE Trans. Magnetics*, 19(6):2514–2519, 1983.

[5] Georges de Rham. *Differentiable manifolds*, volume 266 of *Grundlehren der Mathematischen Wissenschaften [Fundamental Principles of Mathematical Sciences]*. Springer-Verlag, Berlin, 1984. Forms, currents, harmonic forms, Translated from the French by F. R. Smith, With an introduction by S. S. Chern.

[6] M. C. Delfour and J.-P. Zolésio. *Shapes and geometries*, volume 22 of *Advances in Design and Control*. Society for Industrial and Applied Mathematics (SIAM), Philadelphia, PA, second edition, 2011. Metrics, analysis, differential calculus, and optimization.

[7] David J Griffiths. *Introduction to electrodynamics*. Pearson, 2013.

[8] P. Grisvard. *Elliptic Problems in Nonsmooth Domains*. Pitman, Boston, 1985.

[9] W. Hackbusch. *Integral equations. Theory and numerical treatment.*, volume 120 of *International Series of Numerical Mathematics.* Birkhäuser, Basel, 1995.

[10] F. Henrotte, G. Deliege, and K. Hameyer. The eggshell approach for the computation of electromagnetic forces in 2D and 3D. *COMPEL*, 23(4):996–1005, 2004.

[11] F. Henrotte and K. Hameyer. A theory for electromagnetic force formulas in continuous media. *IEEE Transactions on Magnetics*, 43(4):1445–1448, April 2007.

[12] François Henrotte and Kay Hameyer. Computation of electromagnetic force densities: Maxwell stress tensor vs. virtual work principle. *J. Comput. Appl. Math.*, 168(1-2):235–243, 2004.

[13] M. Hinze, R. Pinnau, M. Ulbrich, and S. Ulbrich. *Optimization with PDE constraints*, volume 23 of *Mathematical Modelling: Theory and Applications.* Springer, New York, 2009.

[14] J.D. Jackson. *Classical electrodynamics.* John Wiley, 3rd edition, 1998.

[15] S. McFee, J.P. Webb, and D.A. Lowther. A tunable volume integration formulation for force calculation in finite-element based computational magnetostatics. *IEEE Trans. Magnetics*, 24(1):439–442, 1988.

[16] J.-C. Nédélec. *Acoustic and Electromagnetic Equations: Integral Representations for Harmonic Problems*, volume 44 of *Applied Mathematical Sciences.* Springer-Verlag, Berlin, 2001.

[17] Piyush Panchal and Ralf Hiptmair. Electrostatic Force Computation with Boundary Element Methods. *The SMAI journal of computational mathematics*, 8:49–74, 2022.

[18] S. Sauter and C. Schwab. *Boundary Element Methods*, volume 39 of *Springer Series in Computational Mathematics.* Springer, Heidelberg, 2010.

[19] J. Sokolowski and J.-P. Zolesio. *Introduction to shape optimization*, volume 16 of *Springer Series in Computational Mathematics.* Springer, Berlin, 1992.

[20] Olaf Steinbach. *Numerical approximation methods for elliptic boundary value problems.* Springer, New York, 2008.